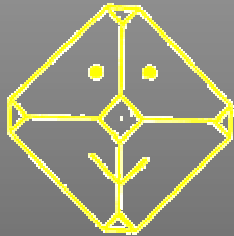




In-situ powder diffraction studies of hydrothermal synthesis and

Hydrothermal synthesis of perovskite materials

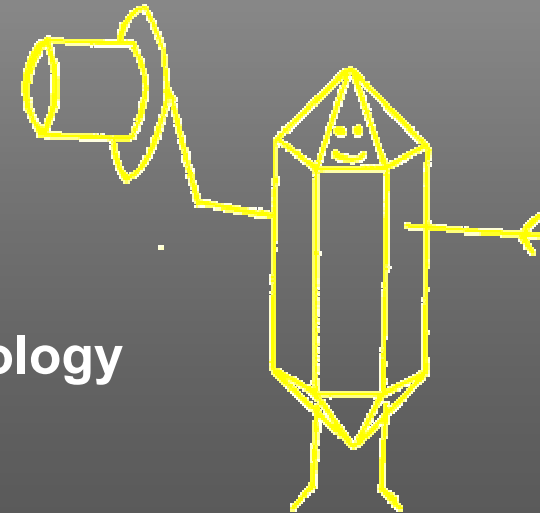
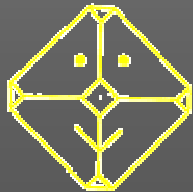


Poul Norby

Department of Chemistry
and

Center for Materials Science and Nanotechnology

University of Oslo, Norway



Examples of in-situ synchrotron X-ray powder diffraction studies

- Hydrothermal synthesis: **zeolites, aluminophosphates, microporous sulfides, mesoporous materials, layered phosphates**
- Chemical reactions: **Sorel cements, carboxylation of phenolates, solid state synthesis,**
- Solid/gas reactions: **high temp. oxidation/reduction**
- Ion exchange
- Intercalation
- Dehydration and dehydroxylation
- Adsorption/desorption
- Thermal transformations
- Structure determination and Rietveld refinement

In-situ studies using synchrotron and conventional X-ray powder diffraction

- Time resolved studies of hydrothermal synthesis of catalytic materials**
- Hydrothermal synthesis of nanomaterials**
- Gas/solid reactions at high temperature**

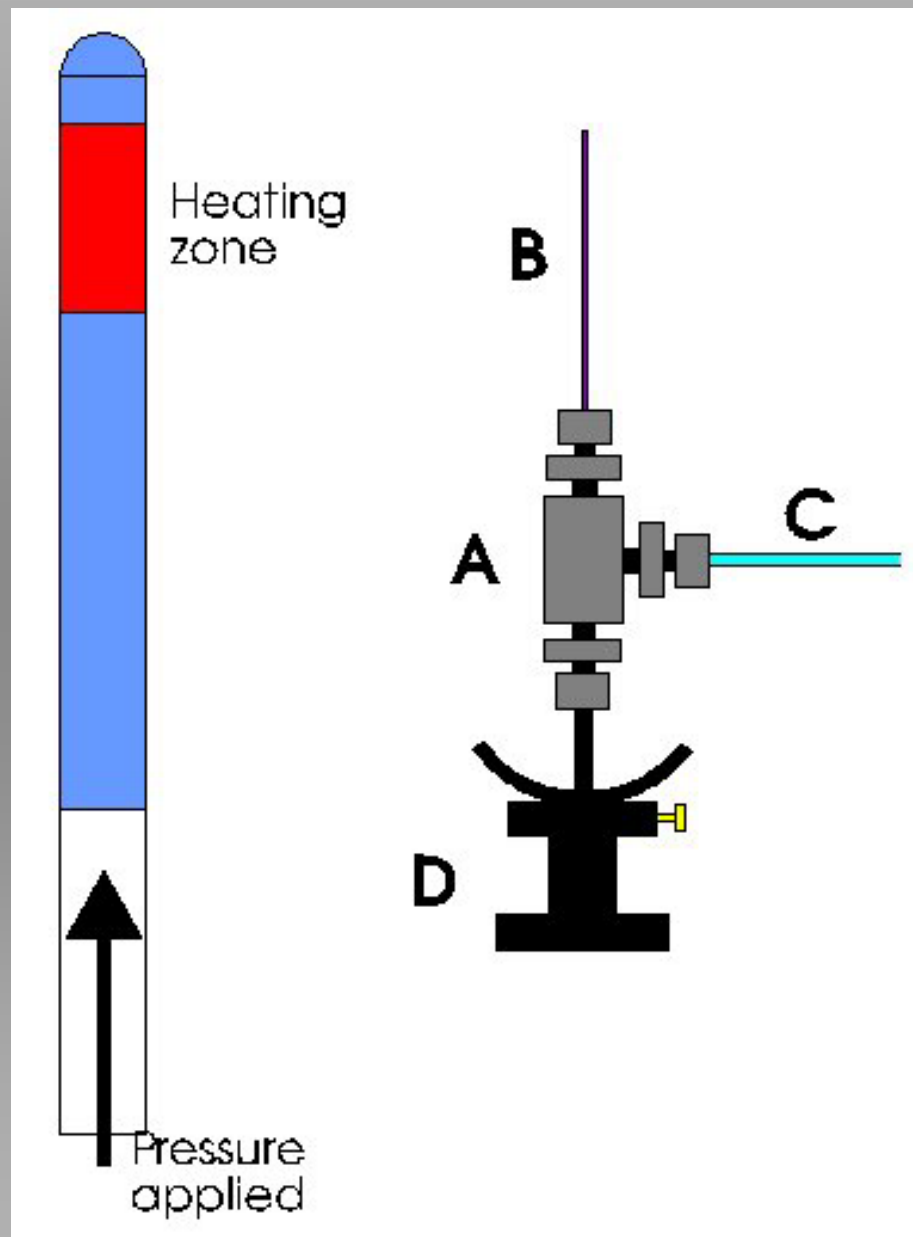
Micro Reaction Cell for In-situ studies of Hydrothermal Synthesis

0.5-0.7 mm quartz glass capillaries

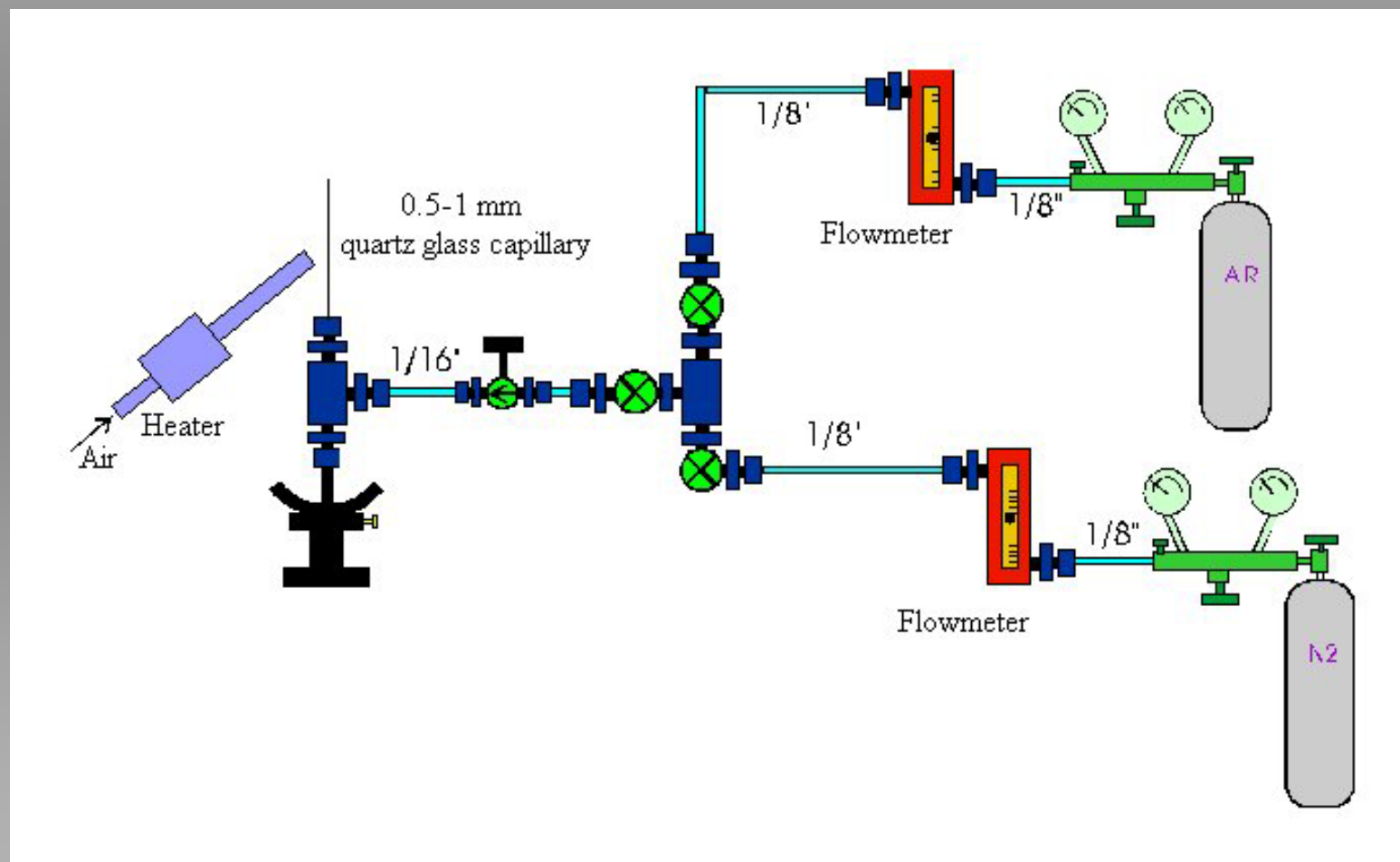
Hot Air Heater

Nitrogen pressure applied

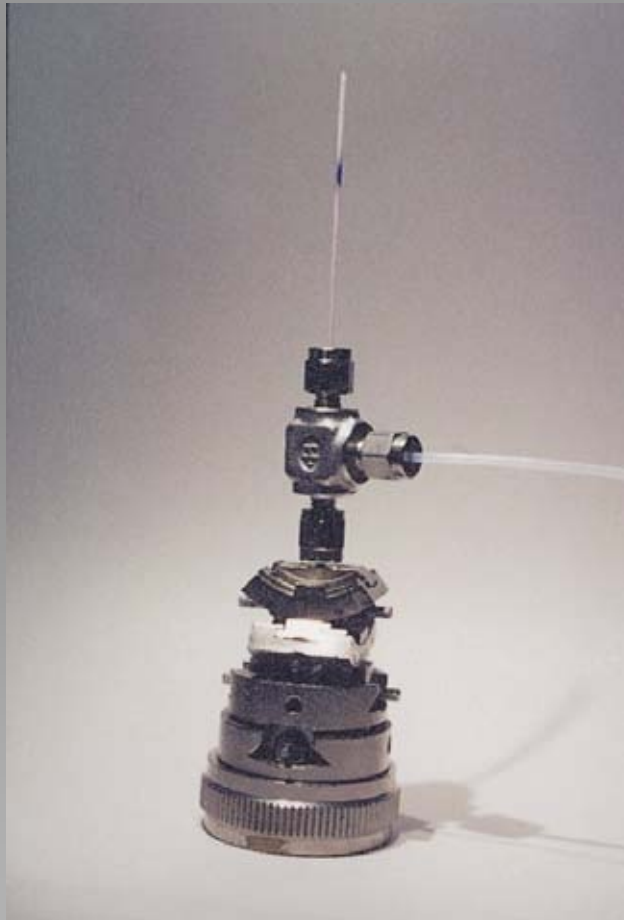
Hydrothermal conditions
up to 260°C (45 atm.)



Micro reaction flow cell for studies of solid-gas reactions



Micro Reaction Cell for In-situ studies of Hydrothermal Synthesis using Synchrotron X-ray Powder Diffraction



The Micro Reaction Cell

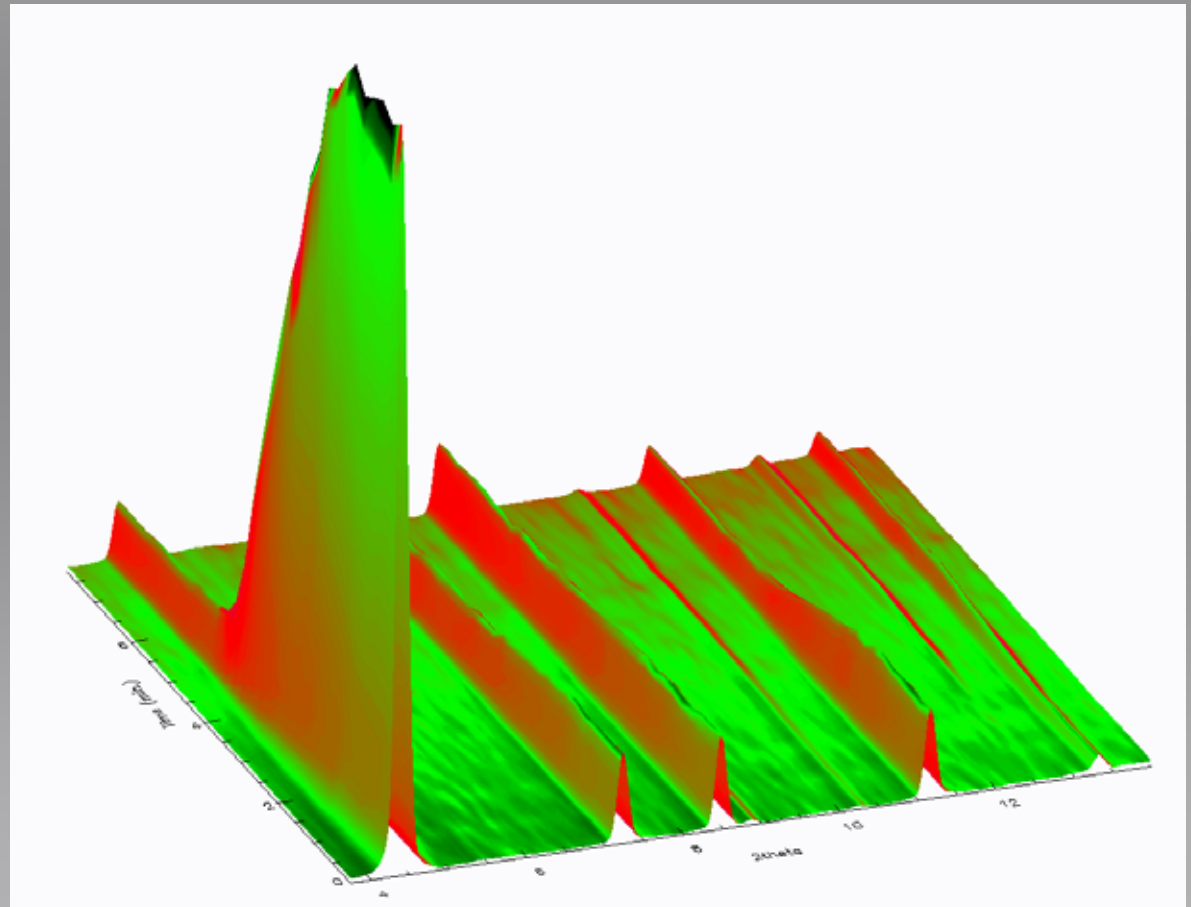
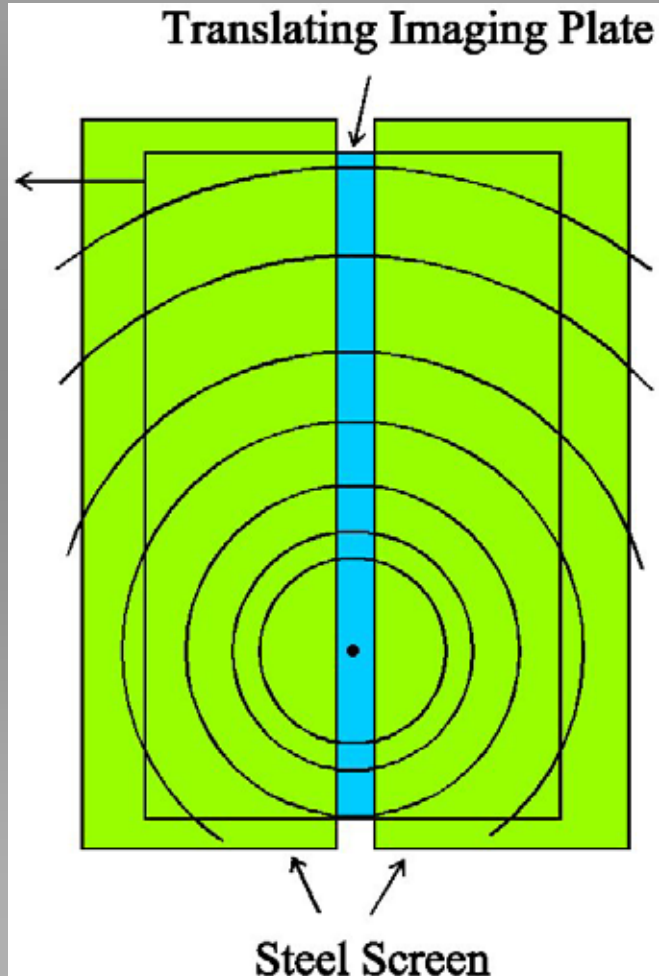


**Mounted at beamline
X7B, NSLS, BNL
with hot air heater**

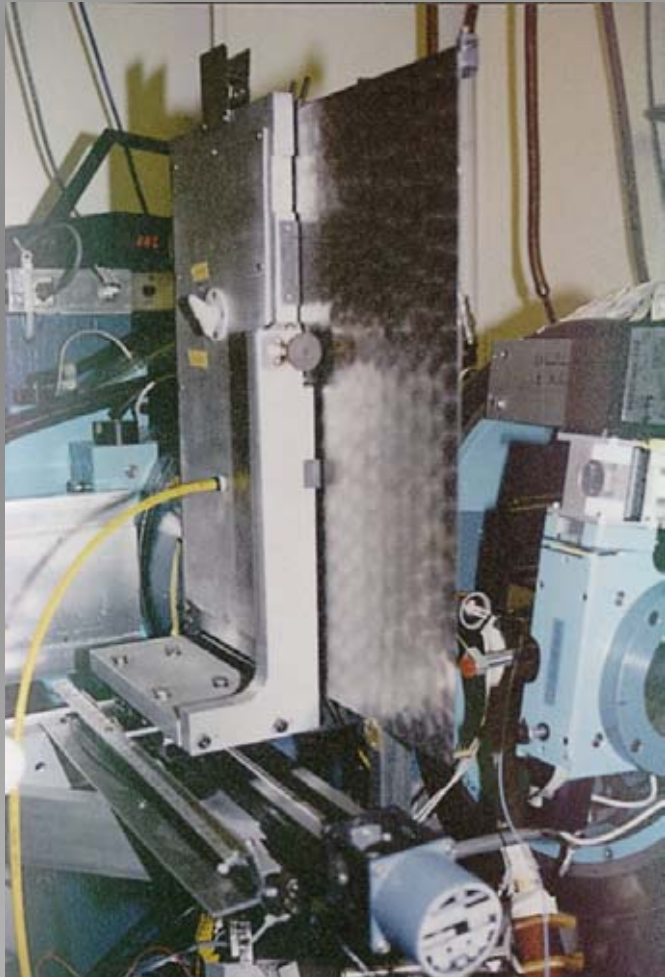


Translating Imaging Plate (TIP) Camera

3-dimensional representation



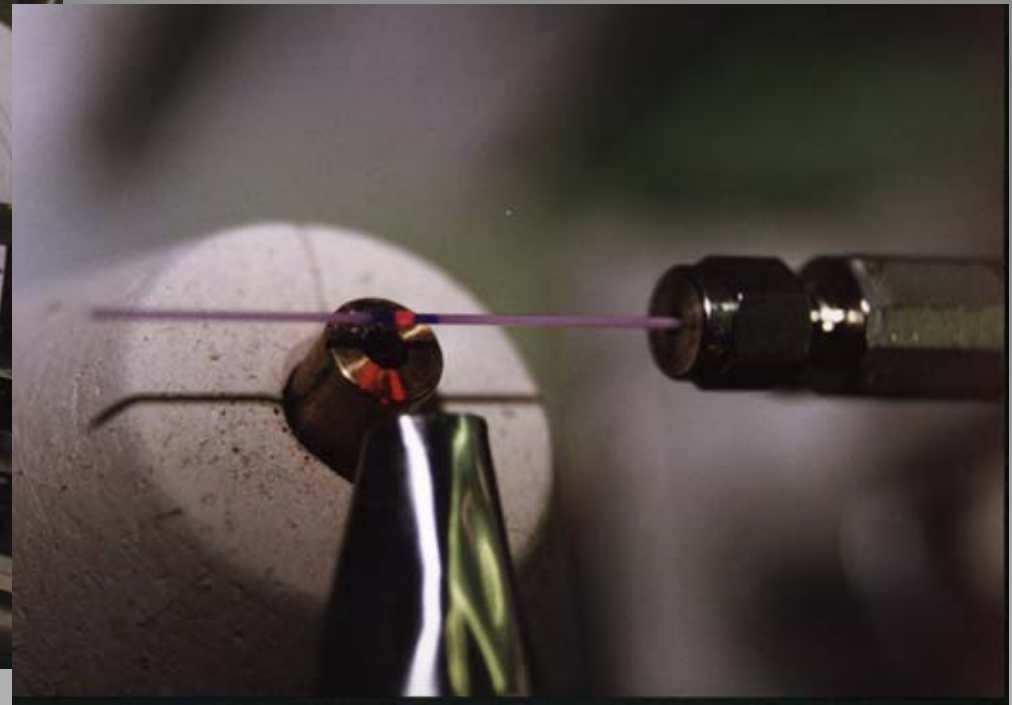
The Translating Imaging Plate (TIP) camera



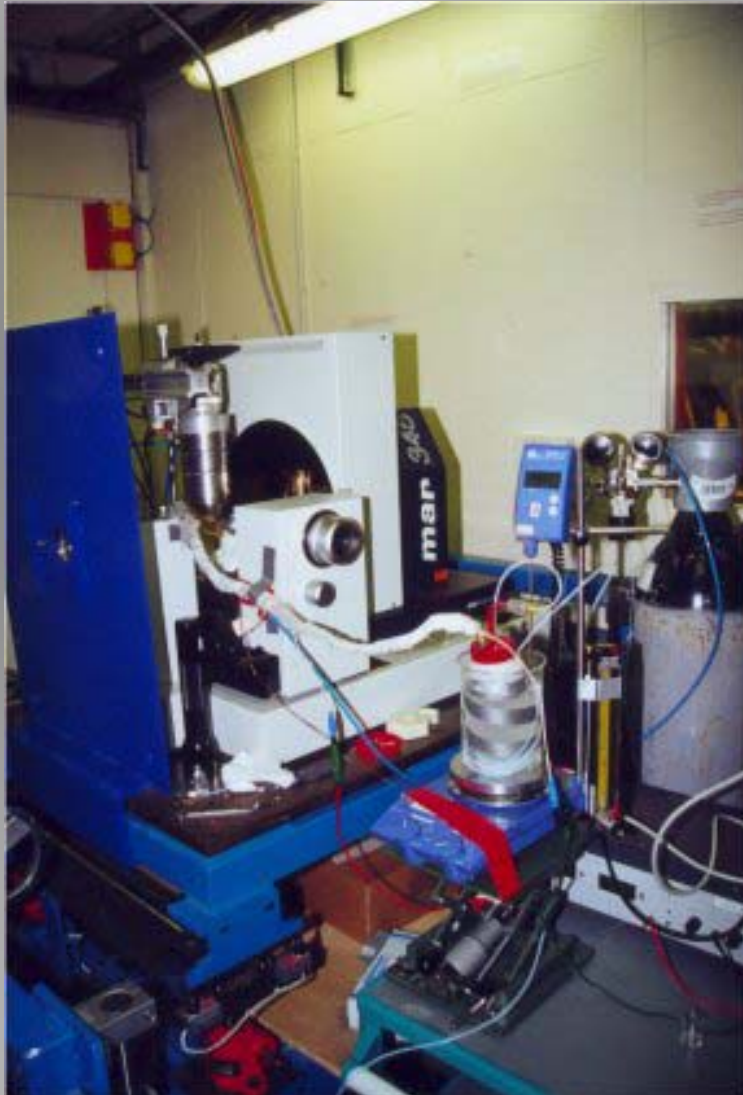
**Rear view of TIP camera
mounted at X7B, NSLS, BNL**



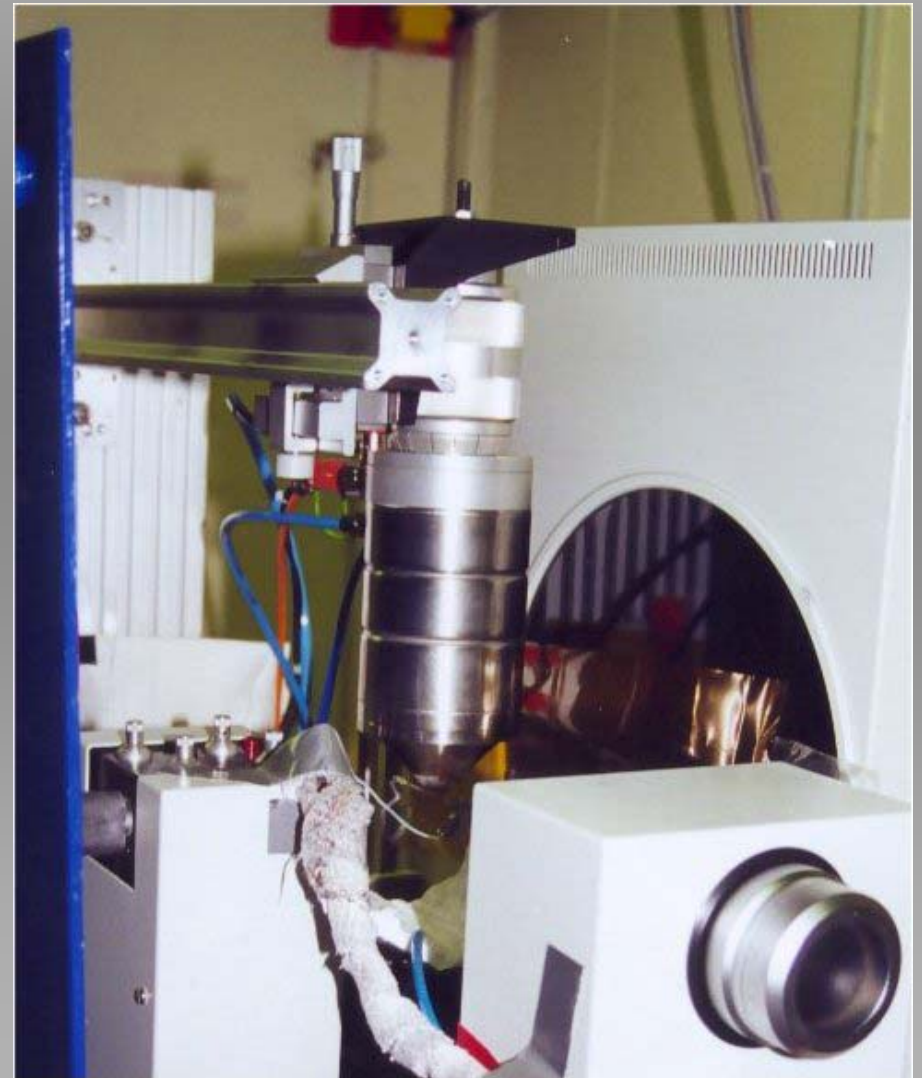
The TIP-II Camera at GILDA, ESRF



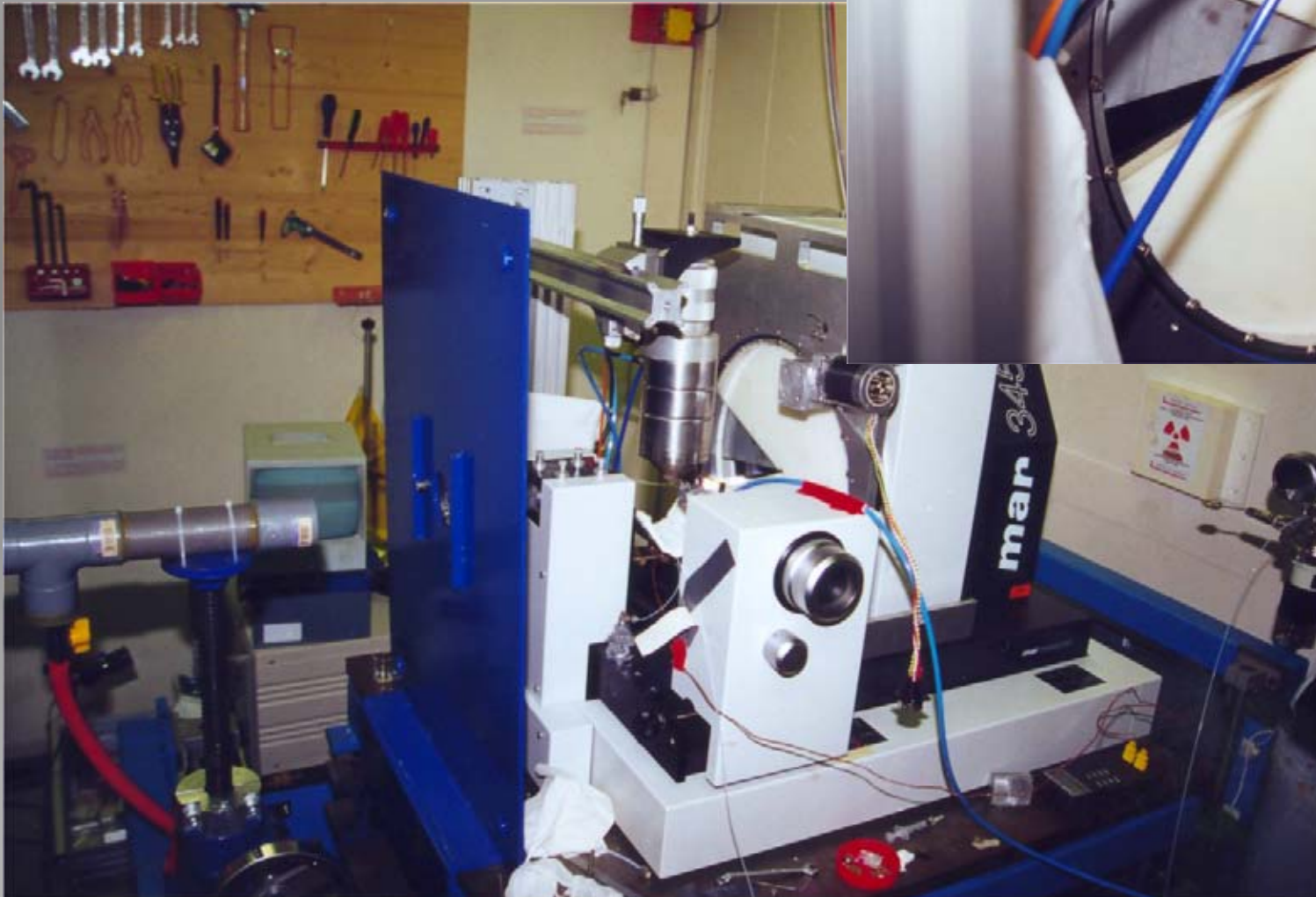
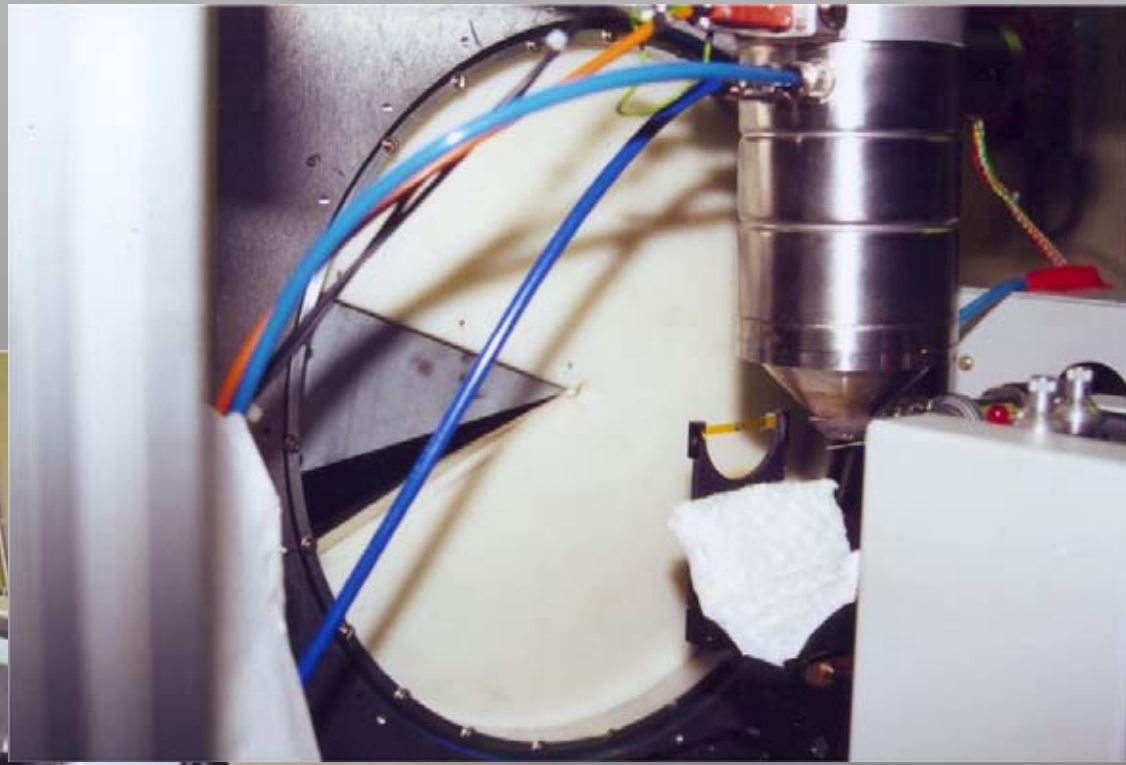
Swiss-Norwegian beamline (SNBL) at ESRF



MAR345 detector
High Temperature heater
Time resolution > 90s



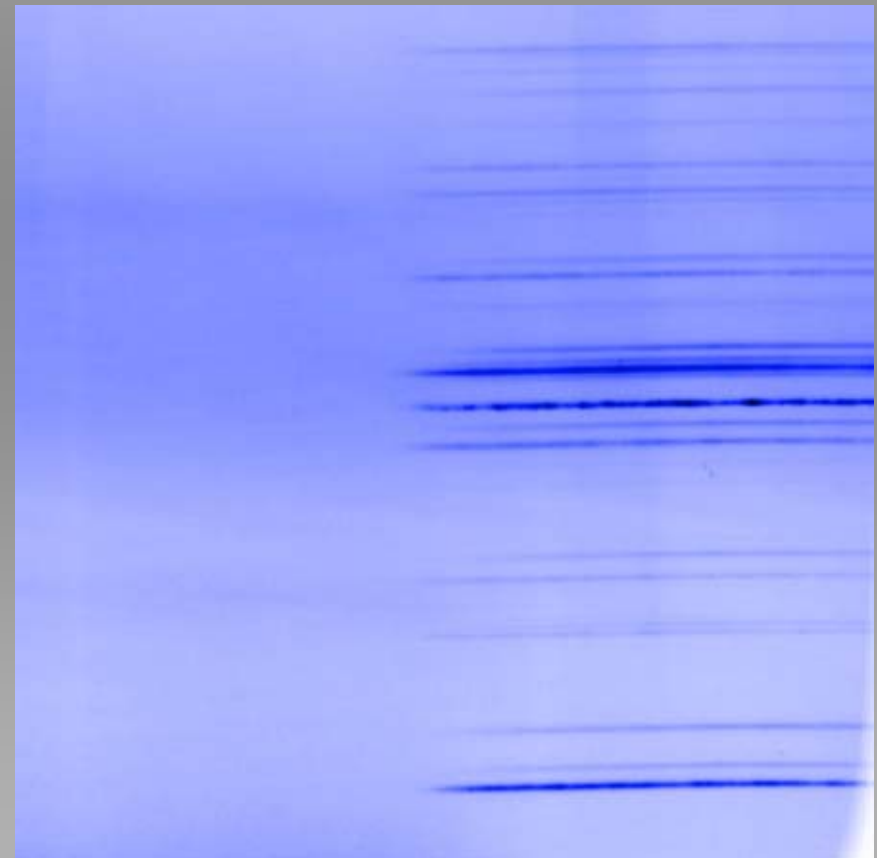
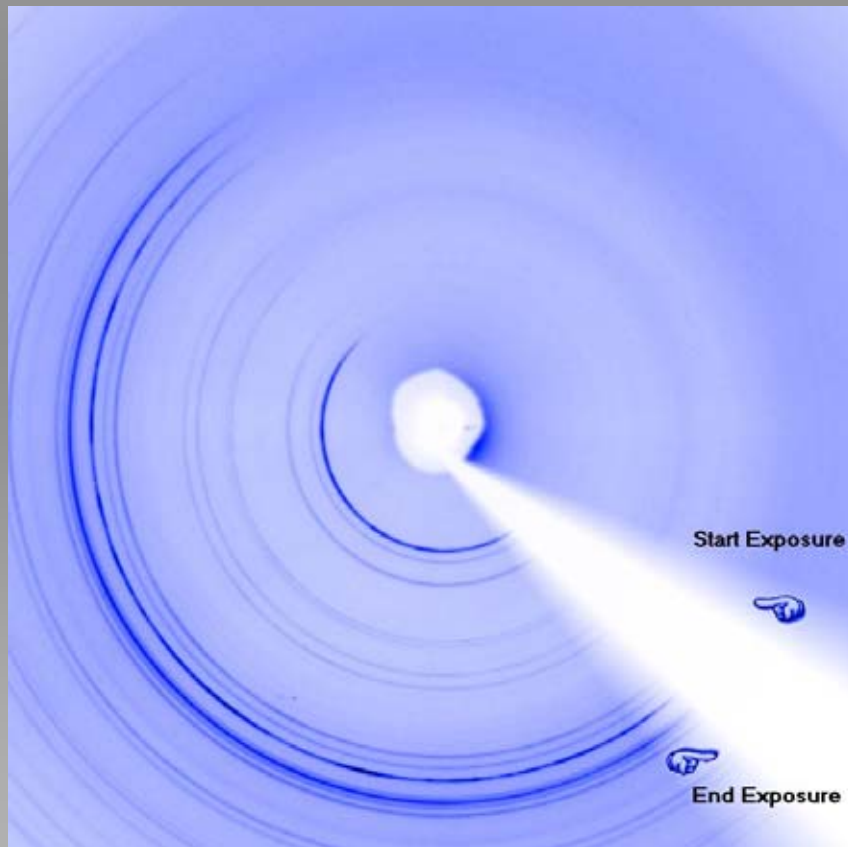
Rotating Slit System MAR345, SNBL



**Time resolution
100ms**

Rotating Slit System, SNBL, ESRF

**Synthesis of cobalt substituted aluminophosphates.
Fast ramp, RT-200°C, 15°C/min**



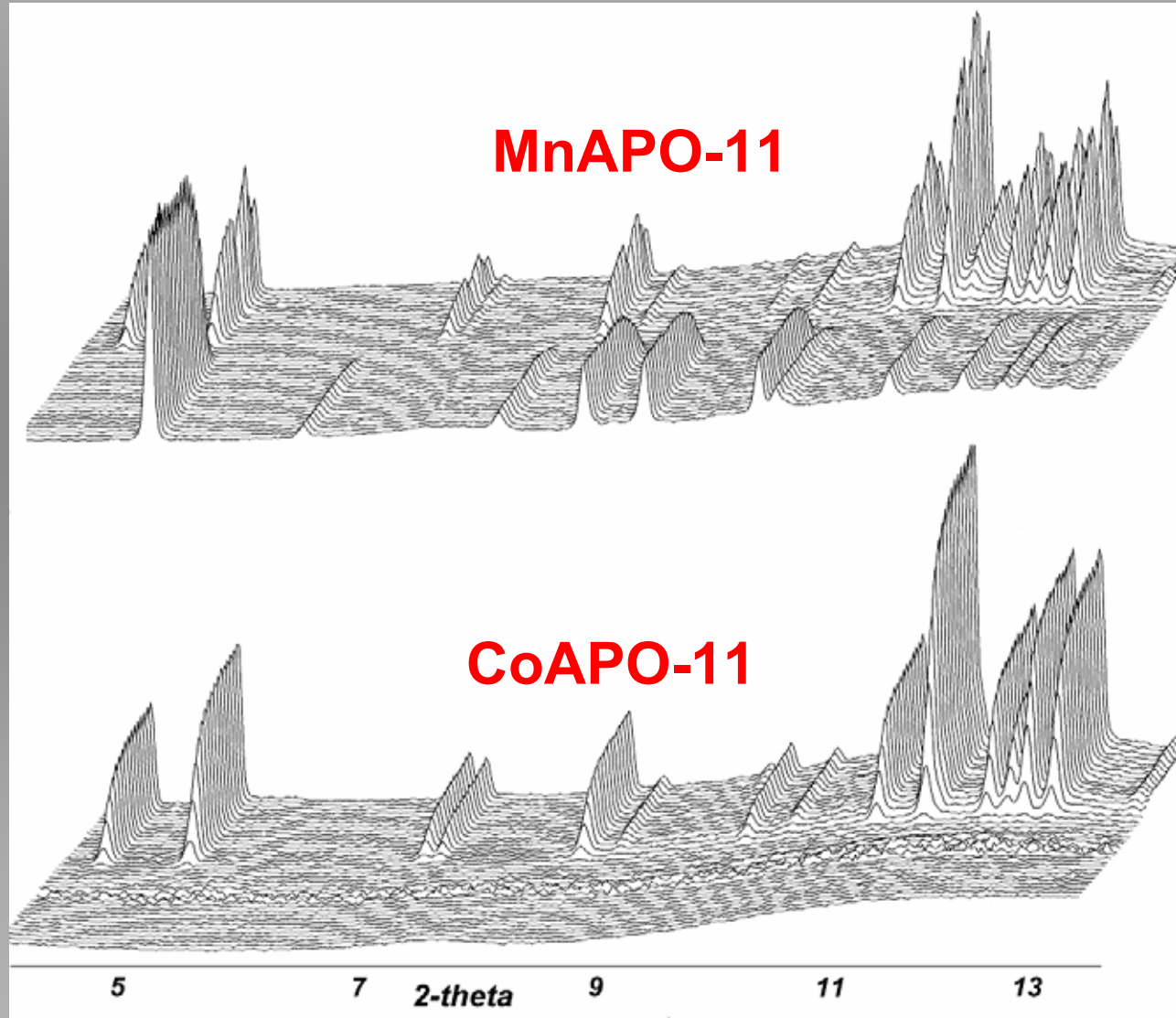
In-situ studies at GILDA

TIP-II camera

GILDA, ESRF

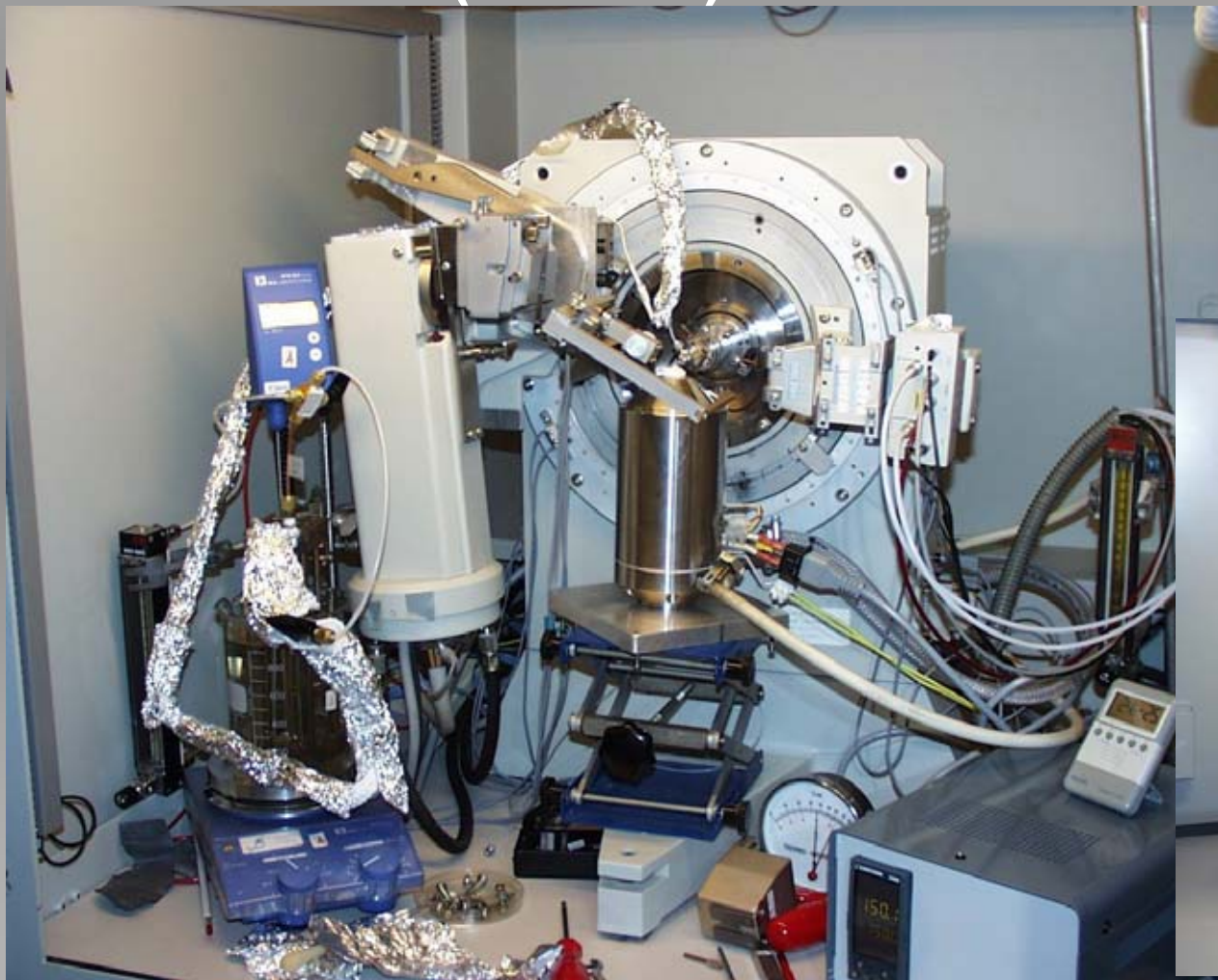
Heating 25-225°C

$$\lambda = 0.8251 \text{ \AA}$$



In-situ studies using conventional X-ray sources.

Siemens (Bruker) D5000



Siemens (Bruker)
GADDS/APEX II



Hydrothermal synthesis of Microporous Aluminophosphates

Kinetic Analysis

Synthesis of transition metal substituted microporous alumino-phosphates from non-aqueous media.

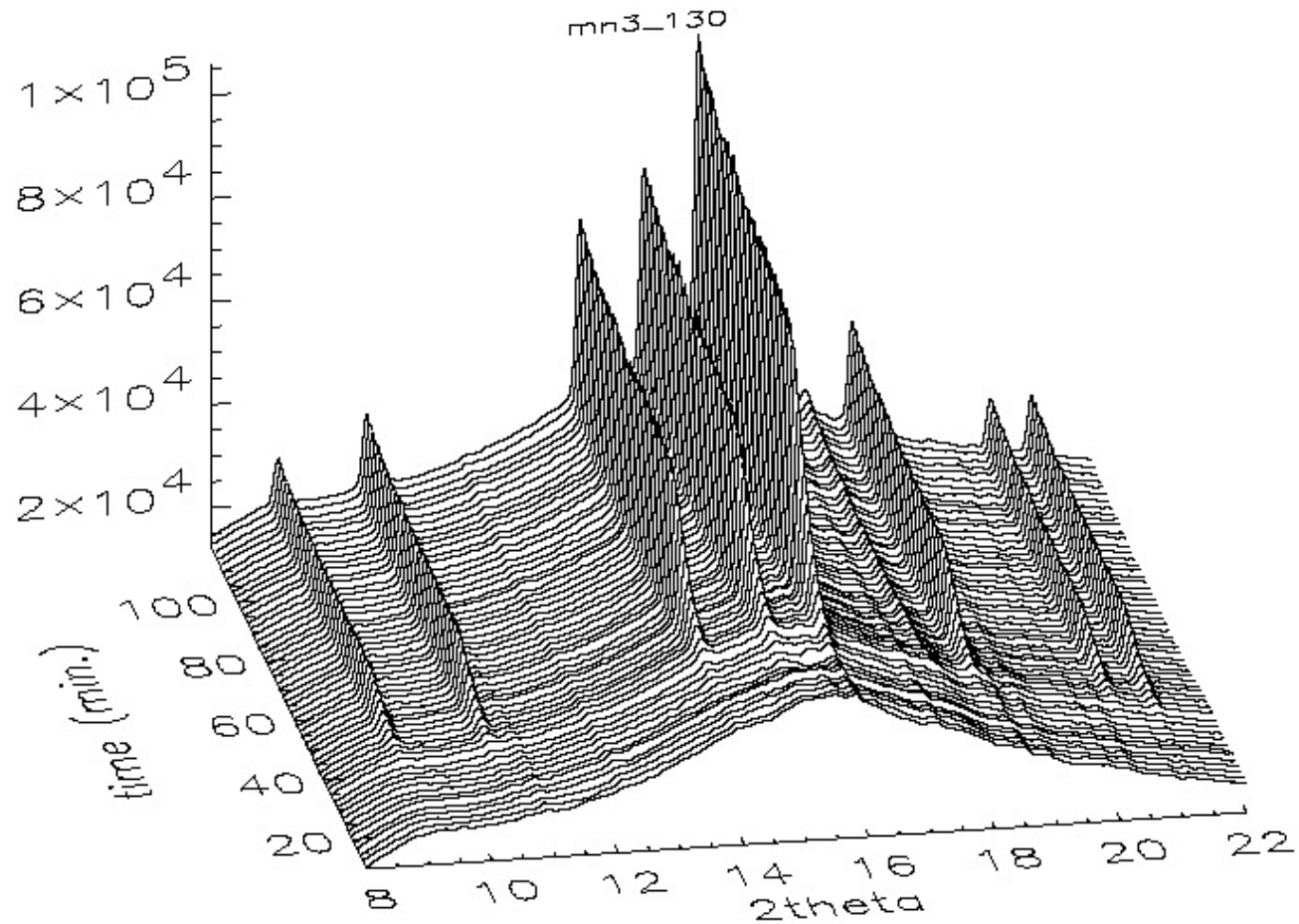
P. Norby et al., *Inorg. Chem.* 38 (1999) 1216-1221

Crystallization of MAPO-5, M = Mn, Co

The effect of mineralizing agents

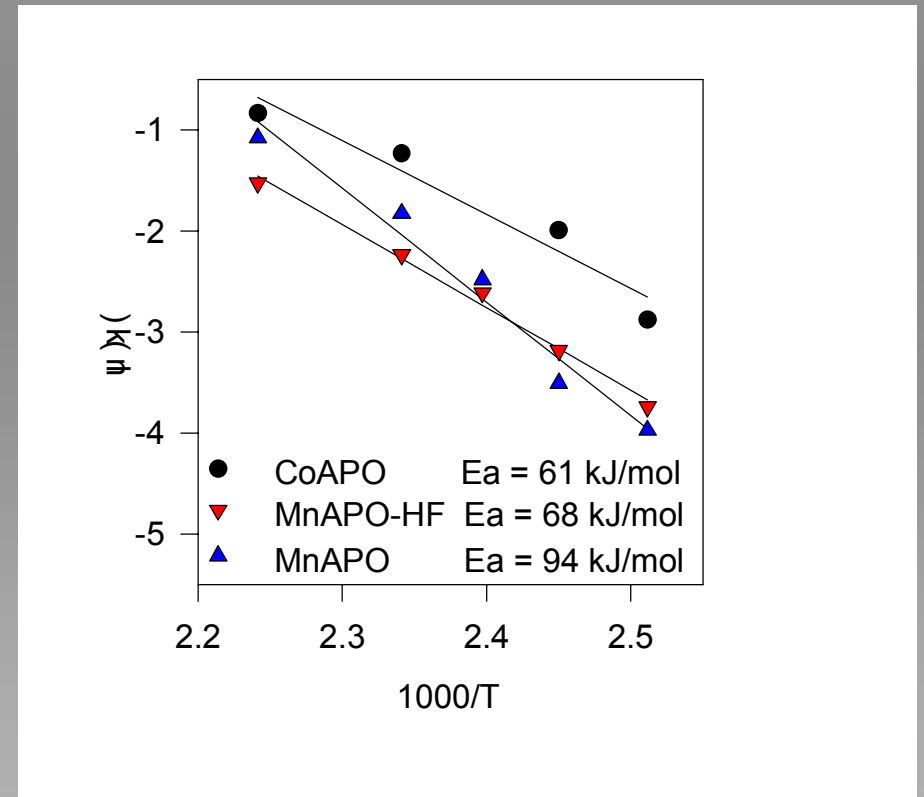
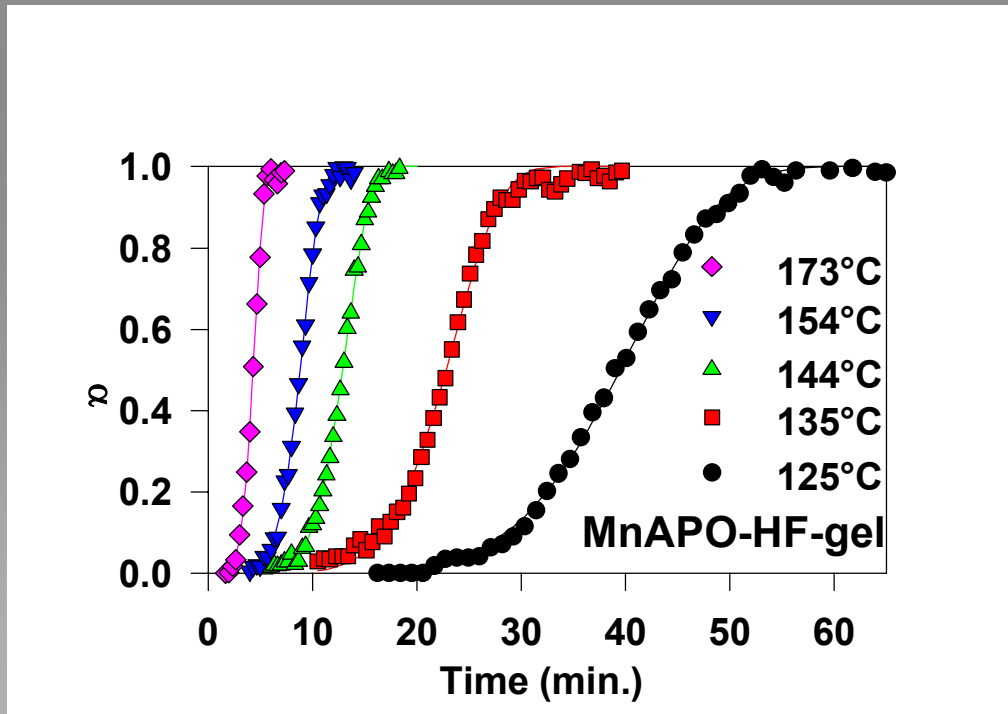
Solvent:	ethylene glycol
Template:	triethylamine, TEA
Al-source:	aluminium isopropoxide
P-source:	85% H₃PO₄
Trans. Metal:	cobalt- and manganese acetates
Mineralizer:	HF
Temperature:	125-180°C

Synthesis of MnAPO-5 at 130°C



Kinetic analysis: MAPO-5 crystallization

Avrami type kinetics expression

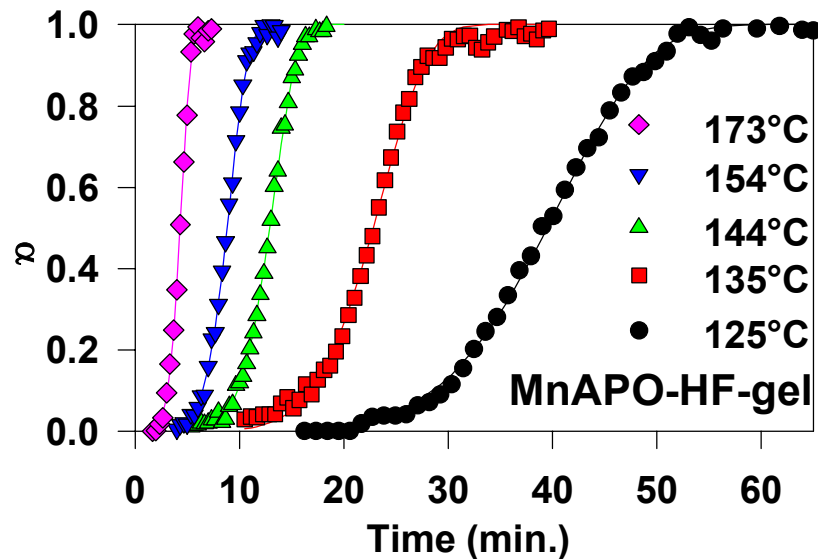


Using the normalized time scale

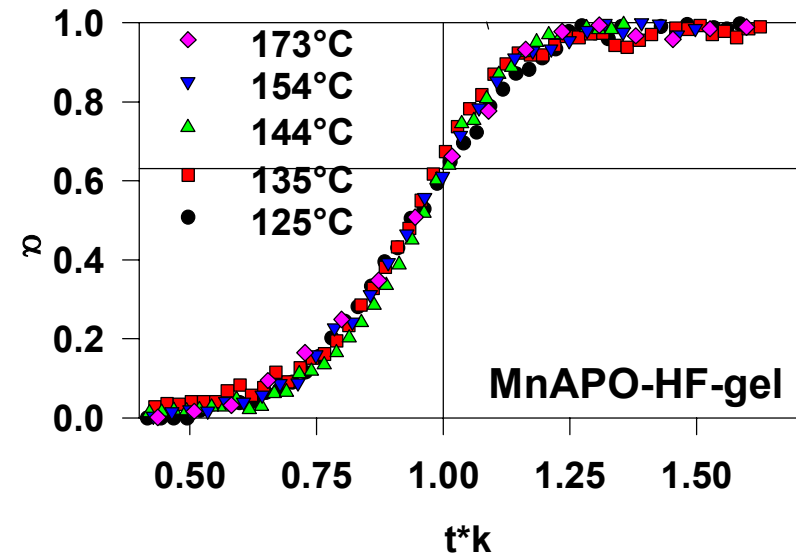
Solvothermal crystallization of MnAPO-5 In-situ synchrotron X-ray powder diffraction

Crystallization curves

Real time



Normalized time



Kinetic analysis using Avrami type expressions.

$$\alpha = 1 - \exp(-(k(t-t_0))^n)$$

- For most applications, the Avrami expression is empirical
- The equation as used most frequently only describes the initial stage of the conversion
- Care must be taken in comparing results obtained using different n-values.

Using $t_{0.63}$ in kinetics analysis

Calculated crystallization curves using constant k .

All curves intersect at:

$$t = 1/k,$$

i.e. $kt=1$ and

$$\alpha = 1 - \exp(-1) = 0.632$$

Thus k may be determined

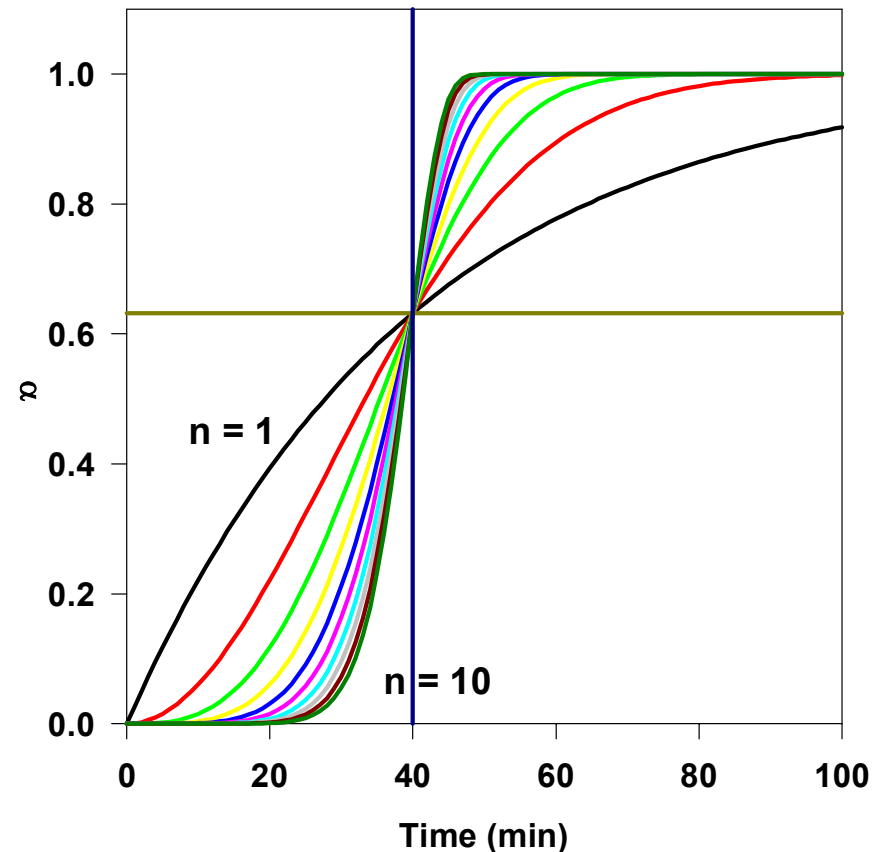
independently of

the value of n

by finding the time where

$$\alpha = 0.63, t_{0.63}$$

$$\alpha = 1 - \exp(-(kt)^n)$$



Synthesis of nanomaterials

- Preparation of free-standing, non-agglomerated, single nanocrystals with size- and morphology control.**
- Mainly hydrothermal and solvothermal synthesis.**

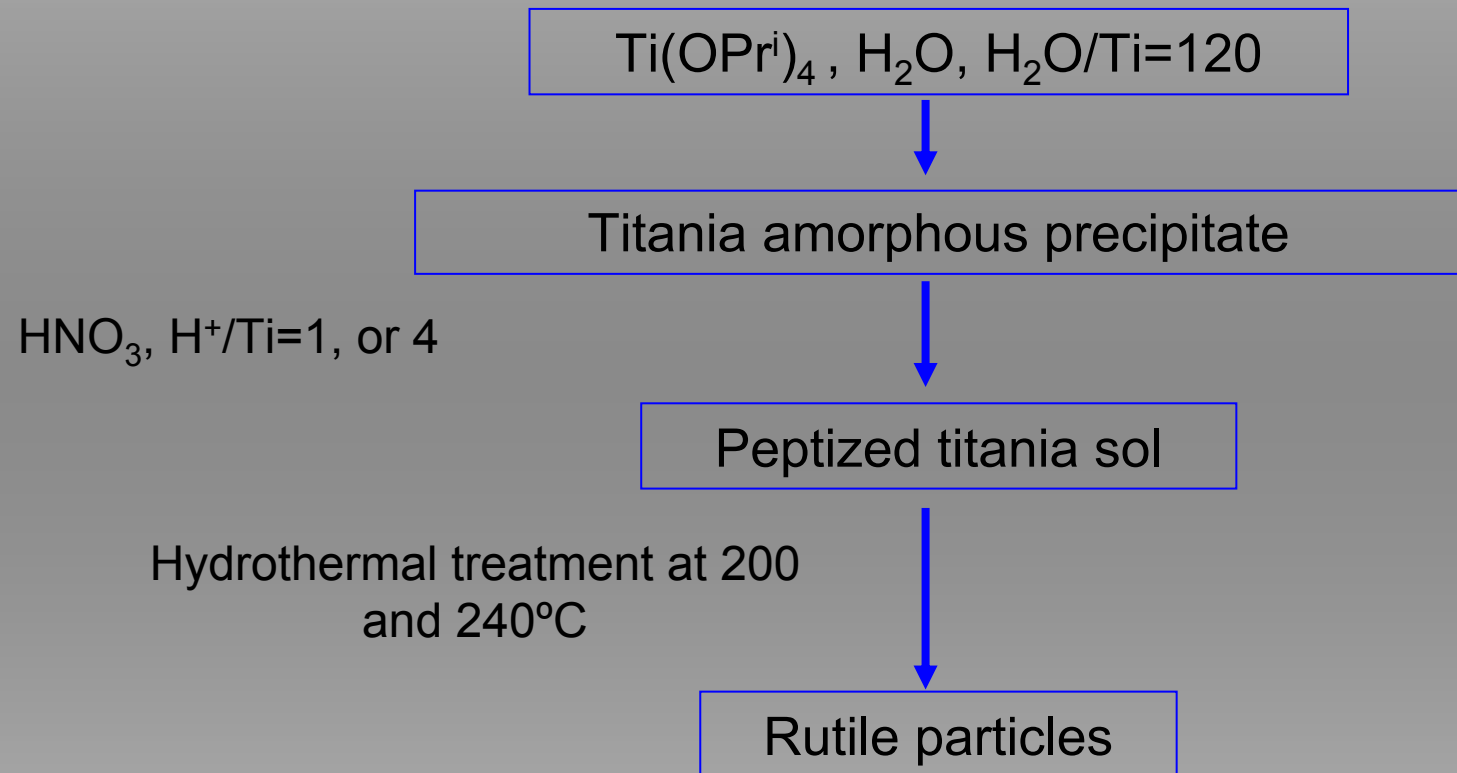
TiO₂ nanocrystals

Juan Yang

- Preparation of rutile nanocrystals; the role of HNO₃ as a peptizer**
- Preparation of anatase nanocrystals from TMAOH, TEAOH, TBAOH peptized sols.**
- Preparation of Ti(Fe)O₂ nanorods**

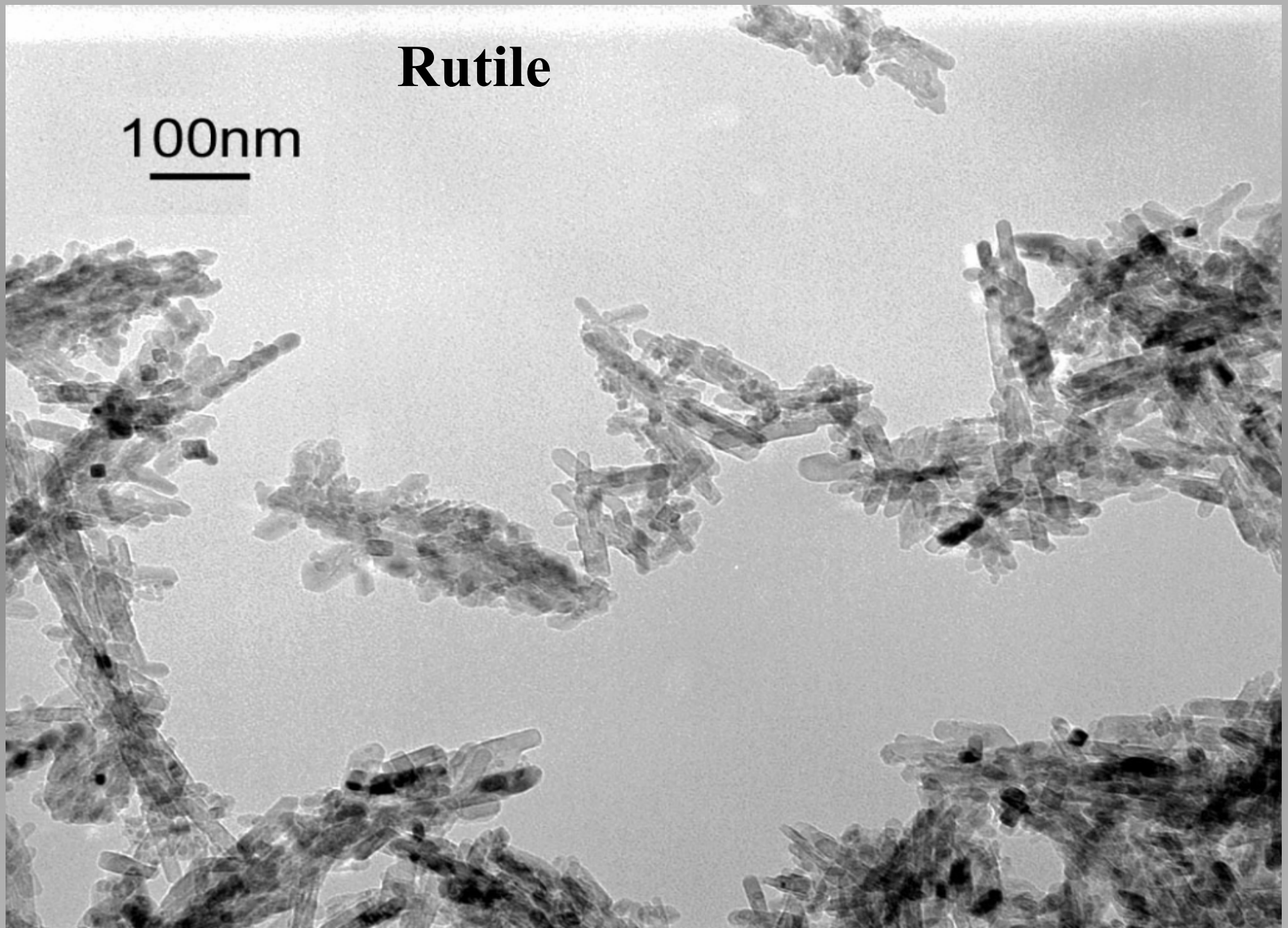
Preparation of rutile nanopowders:

Raw materials: $\text{Ti}(\text{OPri})_4$, HNO_3 , H_2O



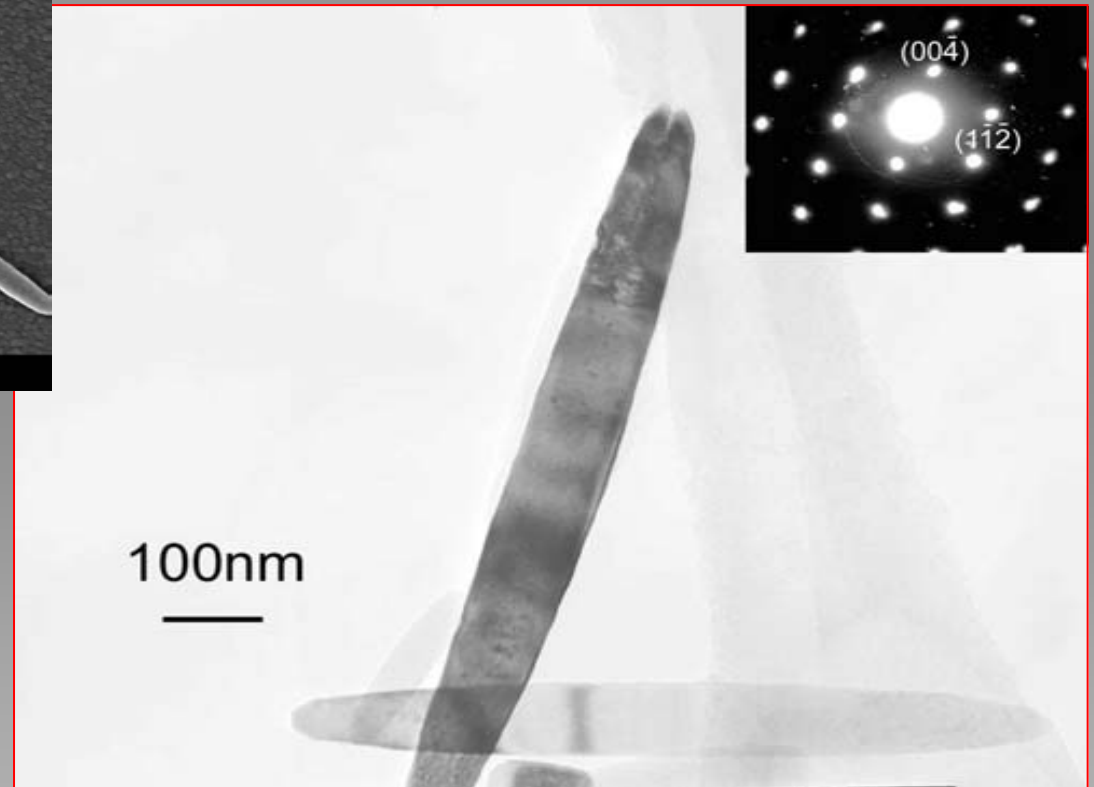
Rutile

100nm

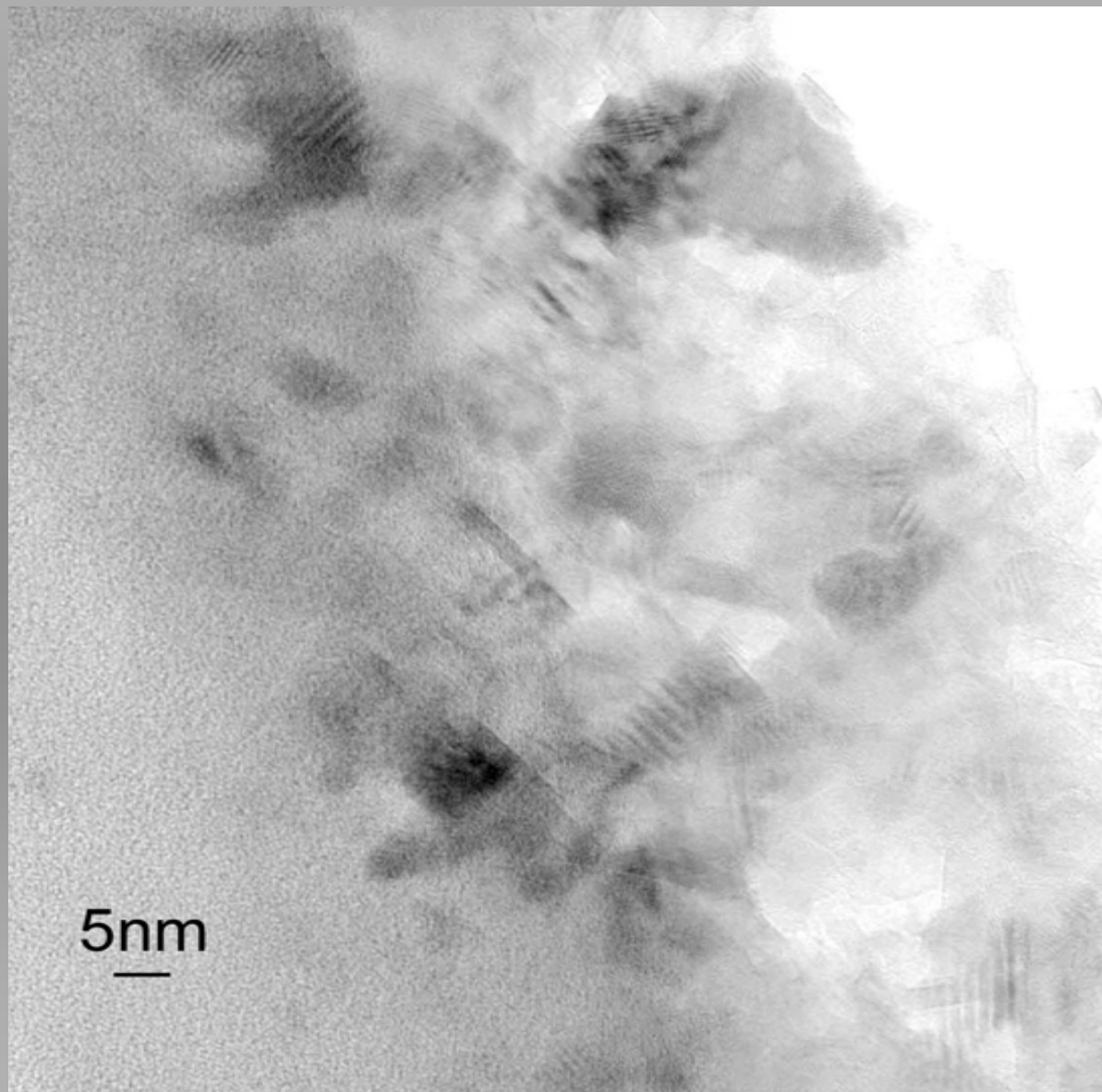


Hydrothermal Synthesis of Fe-doped Anatase (TiO_2) nanorods

TENOH peptized sol
Hydrothermal synthesis



HRTEM morphology of the TENOH-peptized titania sol



Hydrothermal synthesis of Co_3O_4 nanocubes

Starting materials: 0.1M $\text{Co}(\text{NO}_3)_2$ aqueous solution
tetraethylammonium hydroxide
(TENO₄), NaOH,
 $\text{TENO}_4/\text{Co}^{2+}$ ($\text{NaOH}/\text{Co}^{2+}$) = 2, 6 and 8
 NaNO_3

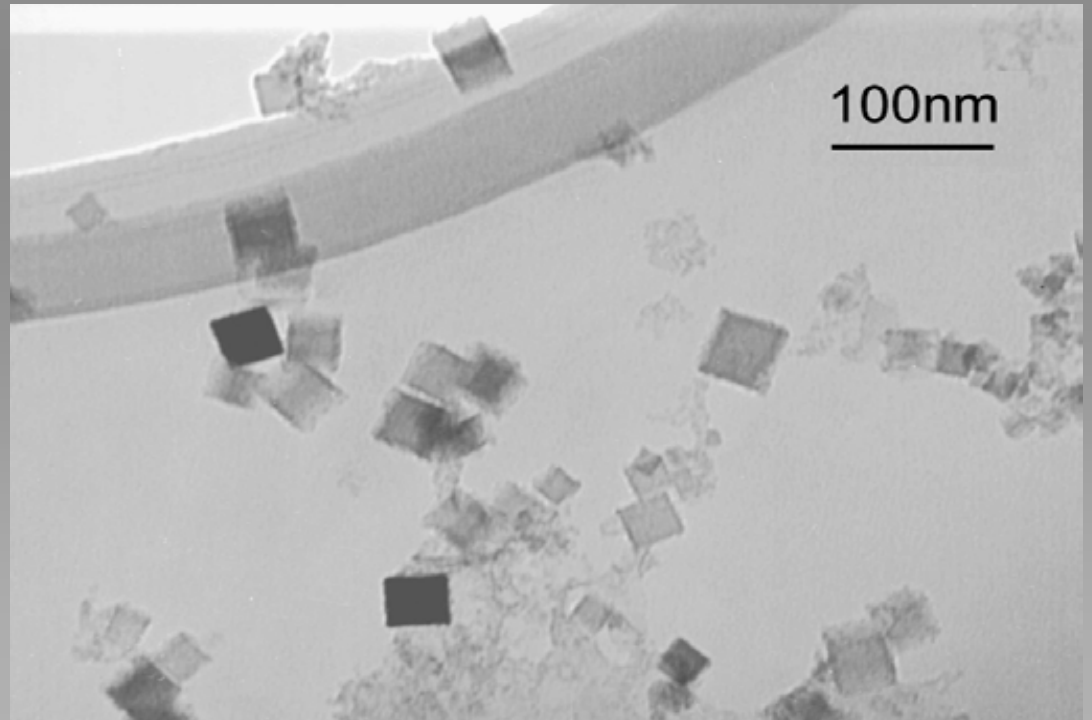
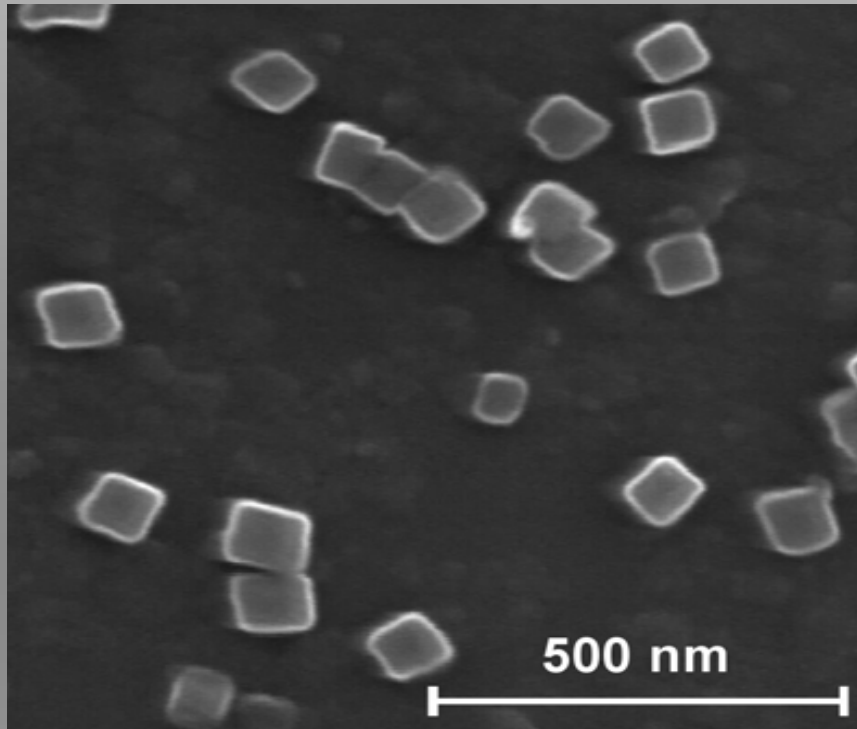
Heated at 80°C for 1.0, 2.5, 4.5 and 6.0 hrs

Hydrothermal treatment at 200°C/2hrs

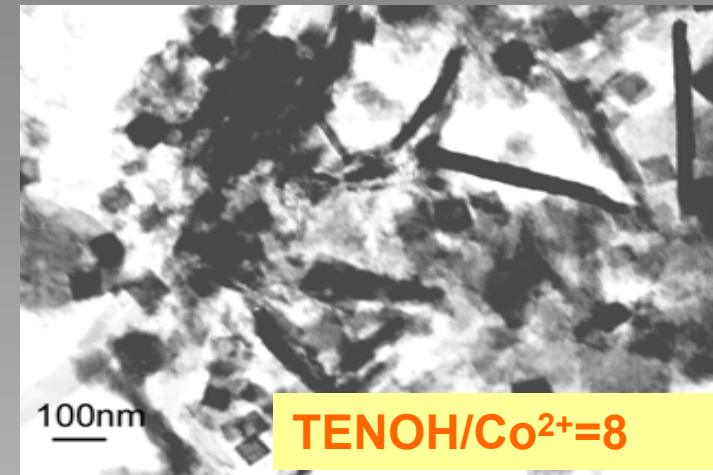
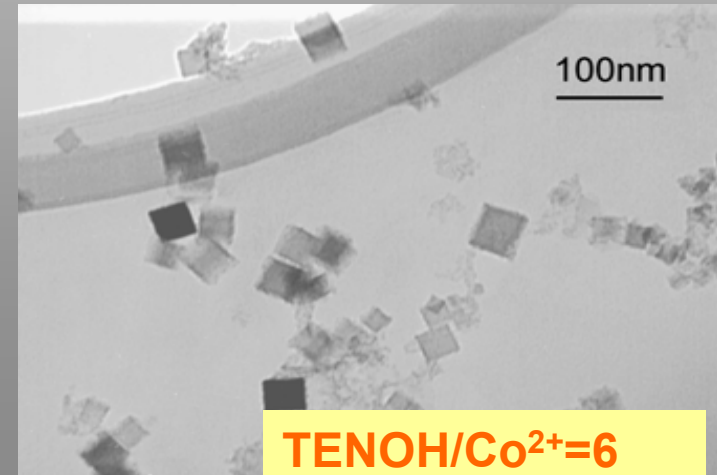
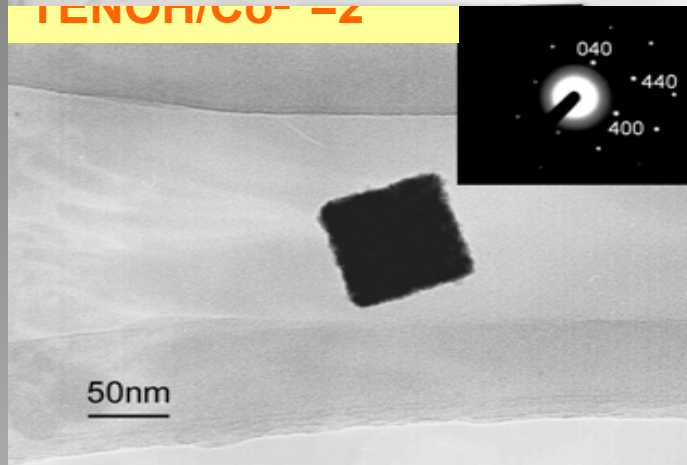
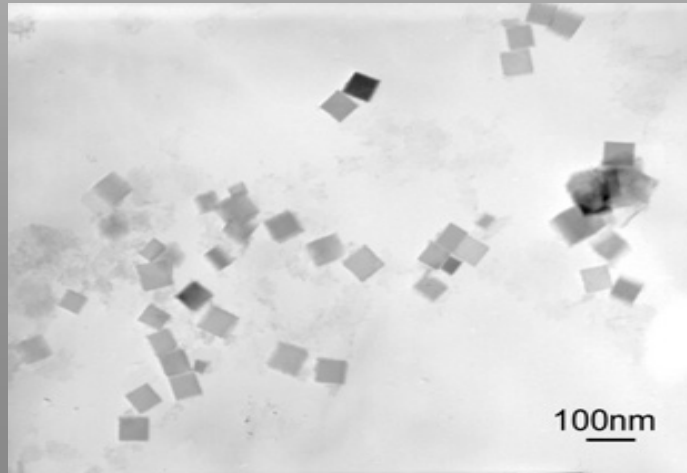
Characterization: XRD, SEM, TEM

News: Hydrothermal synthesis using microwave heating

SEM and TEM images of
 Co_3O_4 nanocubes

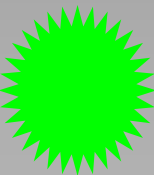
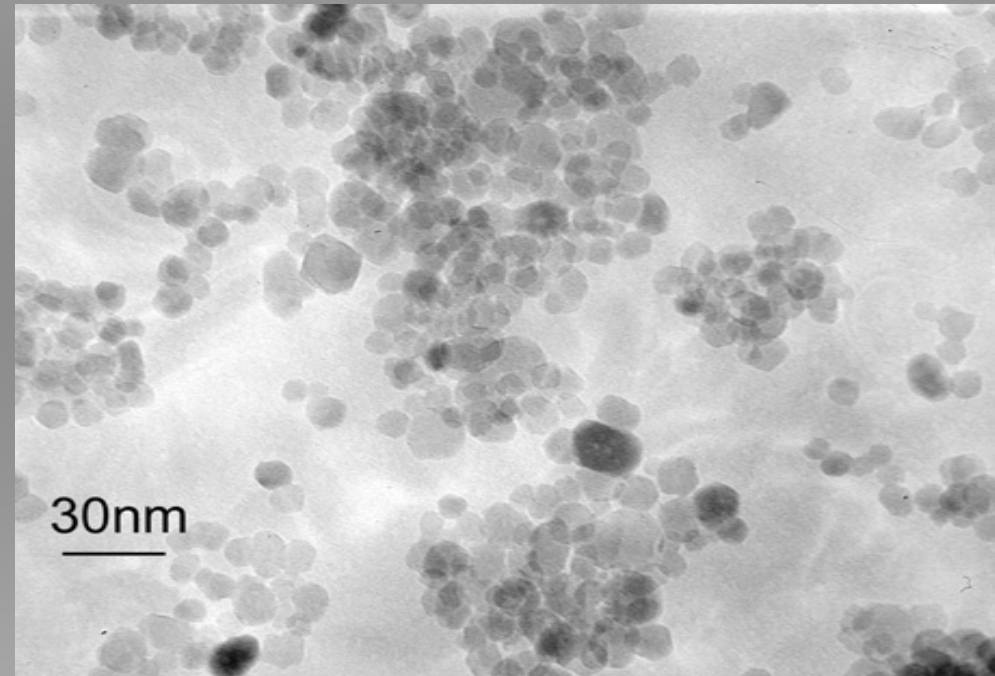
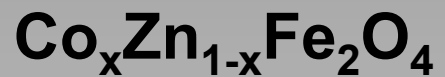
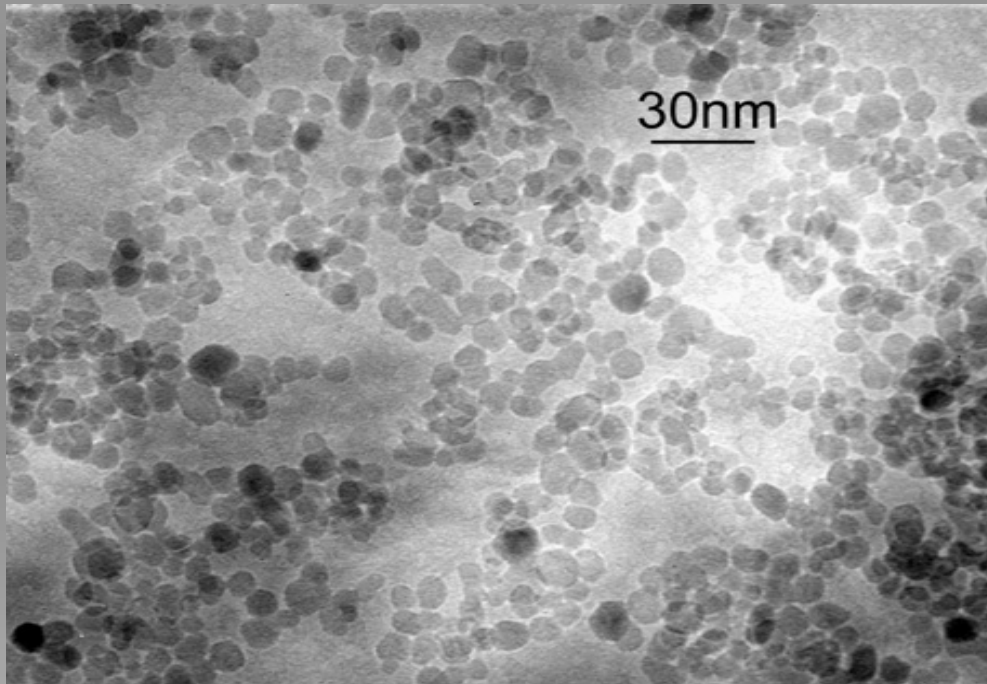


TEM images of the TENOH-peptized powders



Other spinel type oxides

Magnetic properties

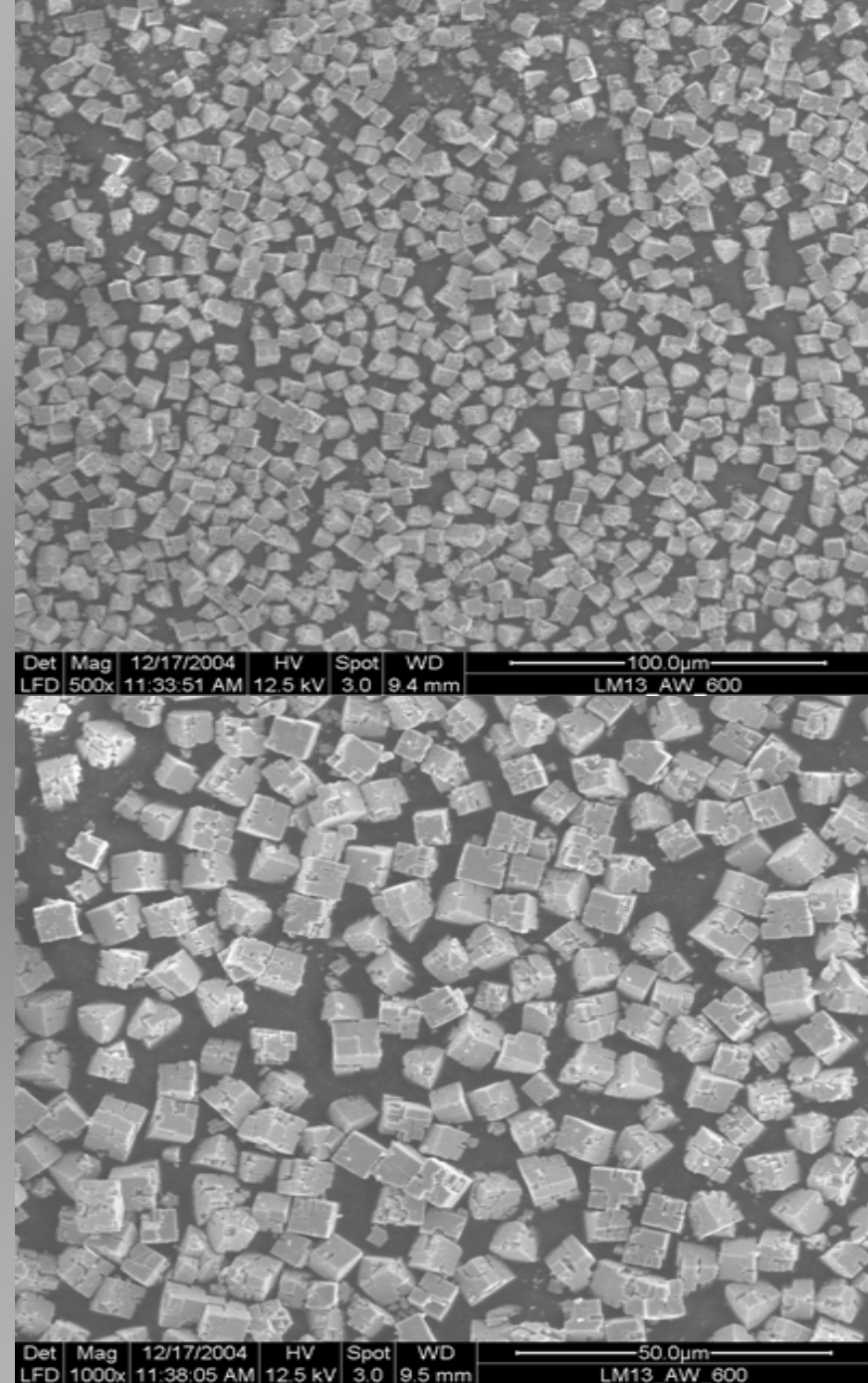
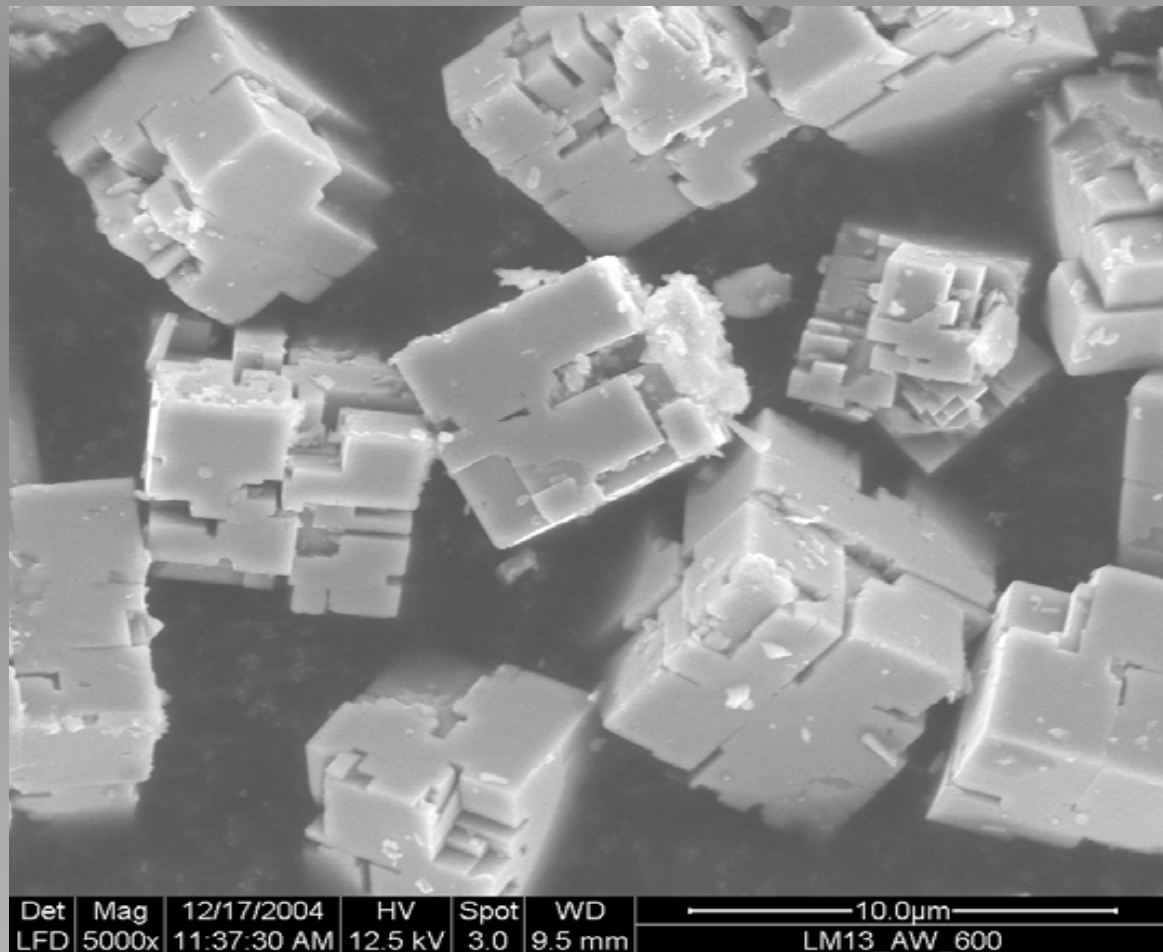


Free-standing perovskite crystals

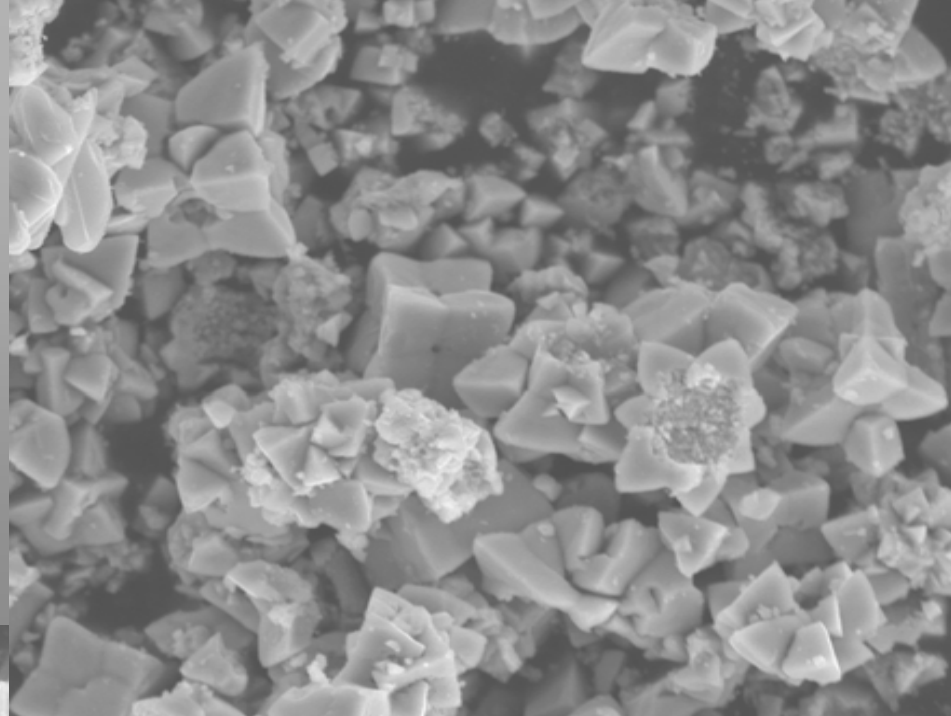
→ Traditional synthesis route; High temperature (Solid state, citrate, combustion, spray pyrolysis...) → agglomerates

→ Hydrothermal synthesis: Very few examples (e.g. BaTiO_3 , hydrothermal)

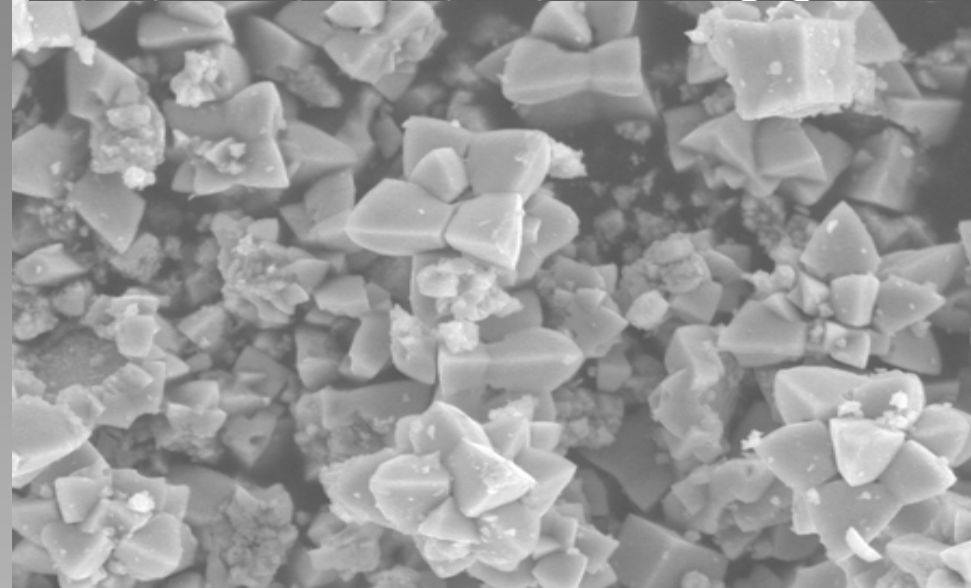
Hydrothermal synthesis: LaMnO_3



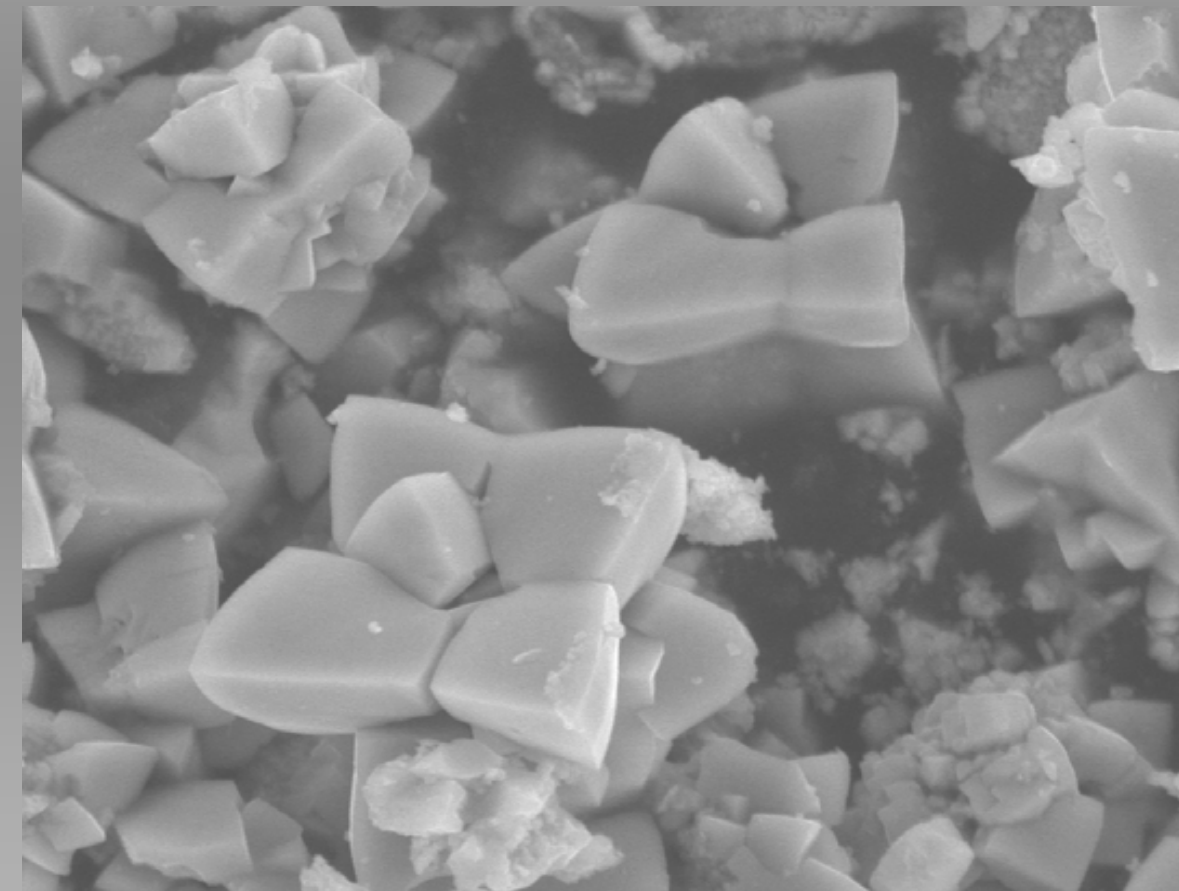
Hydrothermal synthesis: $(\text{La,Sr,Ba})\text{MnO}_{3-x}$



Det	Mag	12/17/2004	HV	Spot	WD	10.0µm
LFD	5000x	11:49:22 AM	12.5 kV	3.0	9.4 mm	LSBM7_AW_600

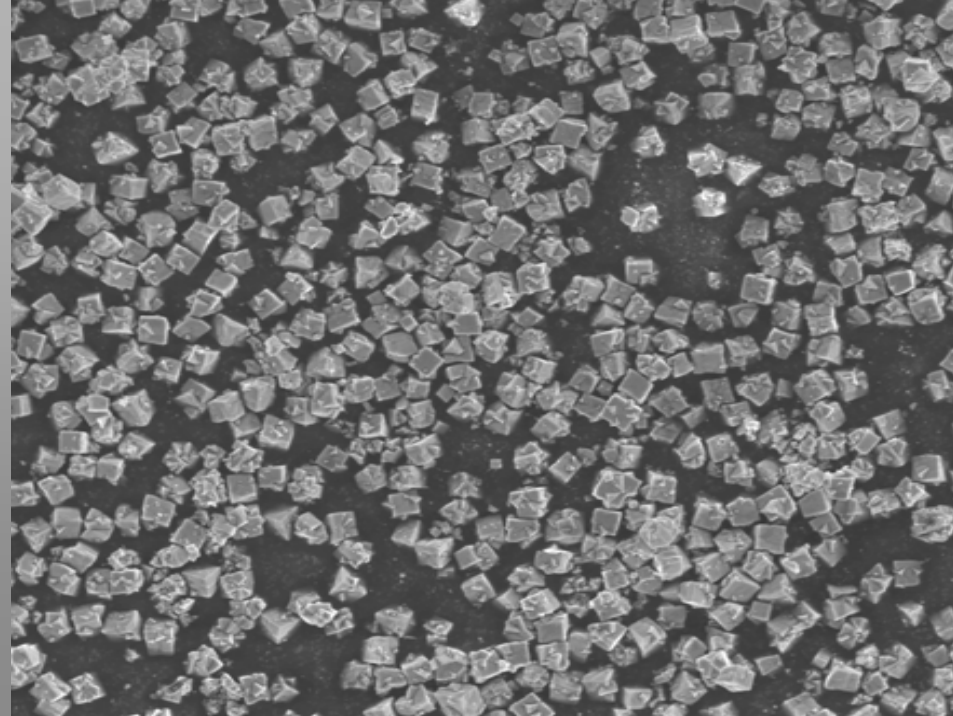


Det	Mag	12/17/2004	HV	Spot	WD	10.0µm
LFD	5000x	11:46:08 AM	12.5 kV	3.0	9.4 mm	LSBM7_AW_600

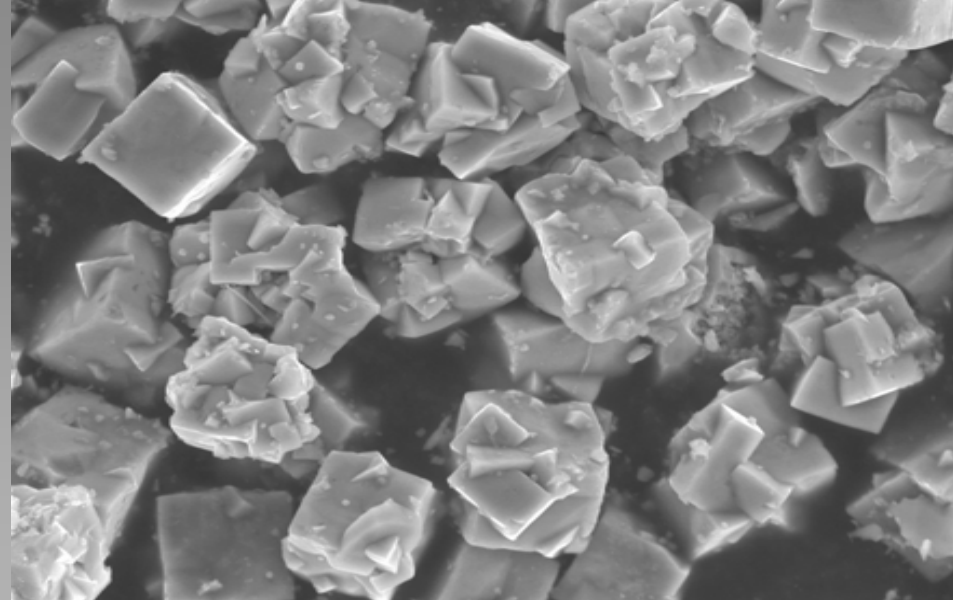


Det	Mag	12/17/2004	HV	Spot	WD	5.0µm
LFD	10017x	11:47:51 AM	12.5 kV	3.0	9.4 mm	LSBM7_AW_600

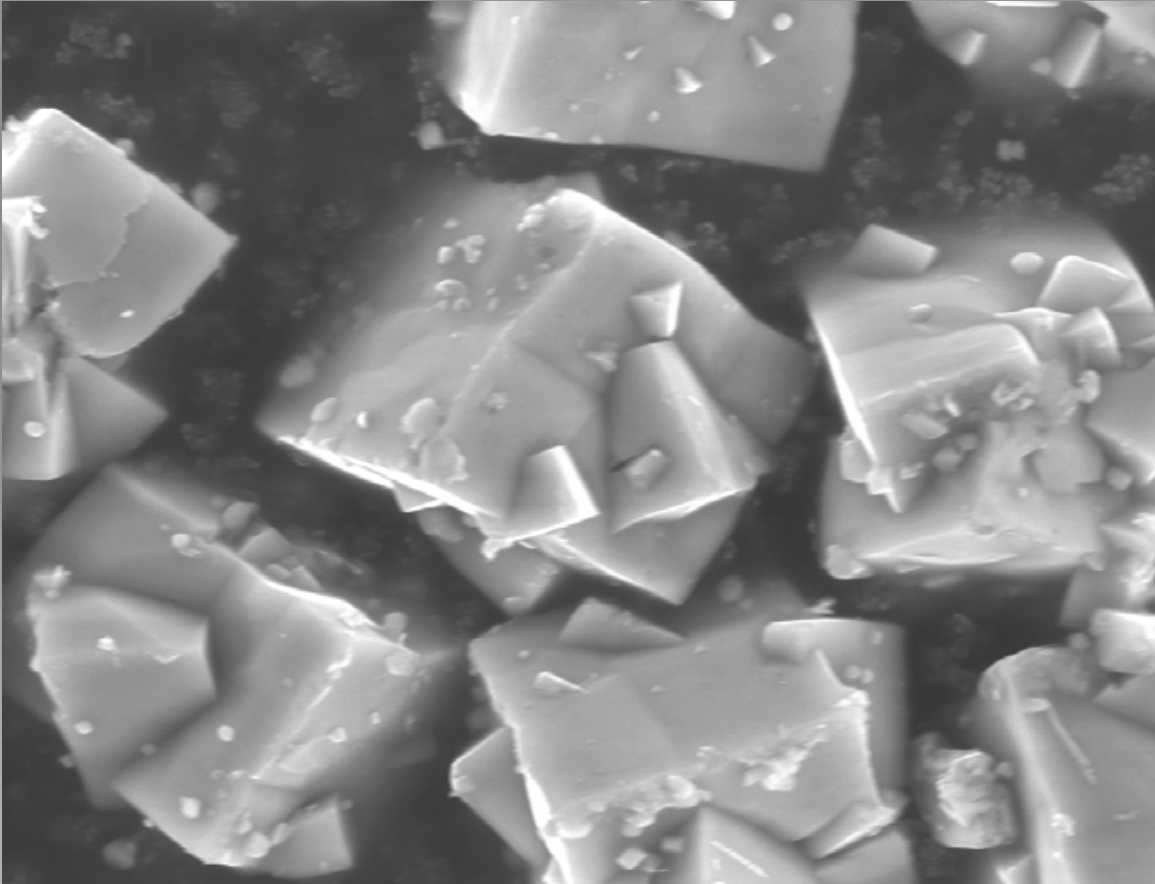
Hydrothermal synthesis: $(\text{La,Sr})\text{MnO}_{3-x}$



Det	Mag	12/17/2004	HV	Spot	WD	50.0µm
LFD	1000x	11:17:35 AM	12.5 kV	3.0	9.4 mm	LSM3_AW_600



Det	Mag	12/17/2004	HV	Spot	WD	10.0µm
LFD	5000x	11:31:45 AM	12.5 kV	3.0	9.4 mm	LSM3_AW_600



Det	Mag	12/17/2004	HV	Spot	WD	5.0µm
LFD	10000x	11:23:50 AM	12.5 kV	3.0	9.4 mm	LSM3_AW_600

Perovskite nano- crystals by hydrothermal methods



Jeffrey J. Urban, Lian Ouyang, Moon-Ho Jo,
Dina S. Wang, and Hongkun Park*
NANO LETTERS 4 (2004) 1547-1550

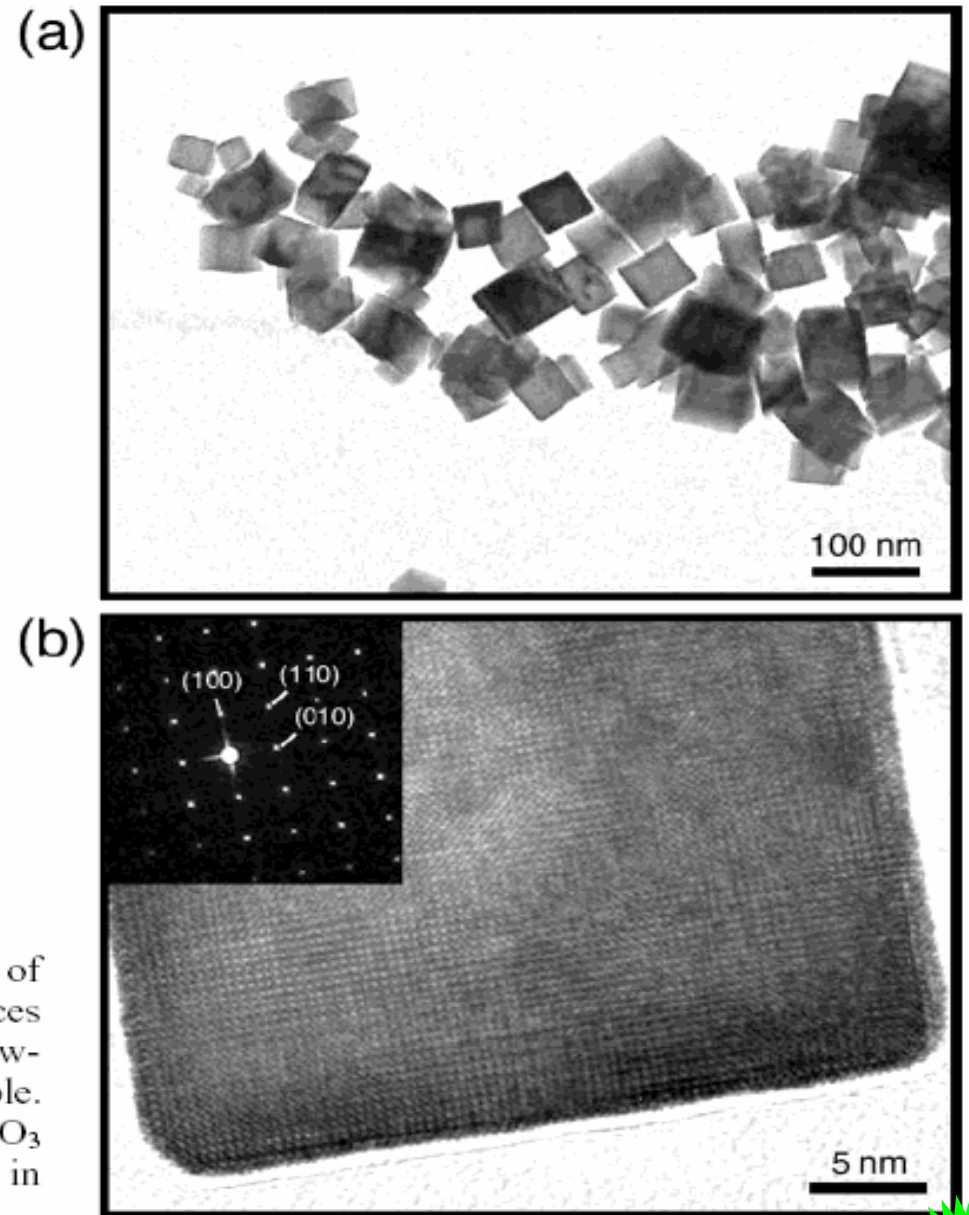
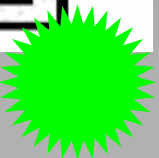


Figure 1. (a) Transmission electron microscopy (TEM) image of $\text{La}_{0.5}\text{Ba}_{0.5}\text{MnO}_3$ nanocubes, illustrating that the reaction produces isolated nanocubes ranging from 20 to 500 nm in size. Low-resolution TEM images for other doping levels are indistinguishable. (b) High-resolution TEM image of a 30-nm $\text{La}_{0.7}\text{Ba}_{0.3}\text{MnO}_3$ nanocube along with a selected area diffraction pattern shown in the inset.



In-situ synchrotron X-ray powder diffraction: Dynamic studies of materials at realistic working conditions.

ESRF

**European Synchrotron
Radiation Facility**

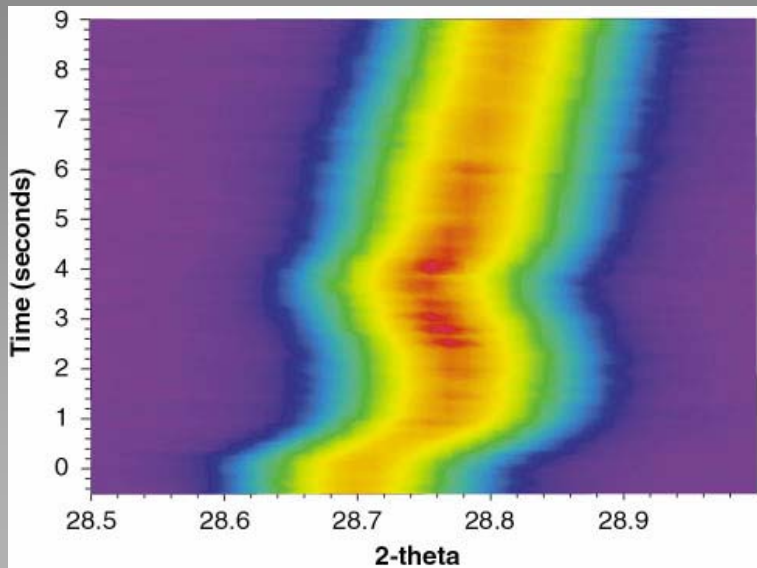
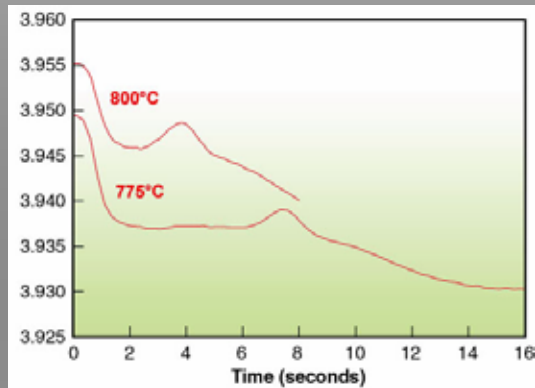
Grenoble

**Swiss/Norwegian beam line:
SNBL**

**Materials Science beamline:
ID11**

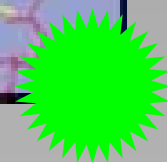


Highlights 2001



ESRF
European Synchrotron
Radiation Facility

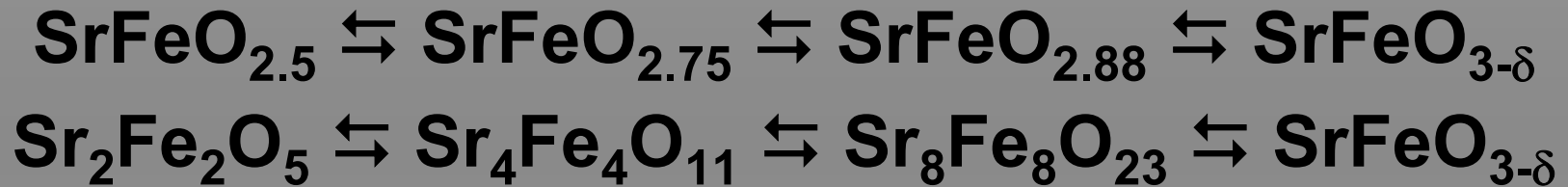
Highlights 2001



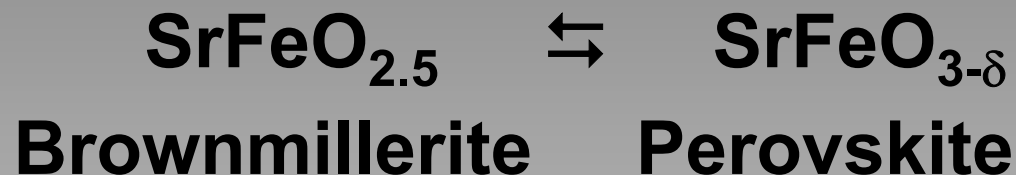
Oxygen permeable membranes at operating conditions

High Temperature Oxidation/Reduction of materials for oxygen permeable membranes

Material: $\text{SrFe}_{0.97}\text{Cr}_{0.03}\text{O}_{3-\delta}$



High Temperature:



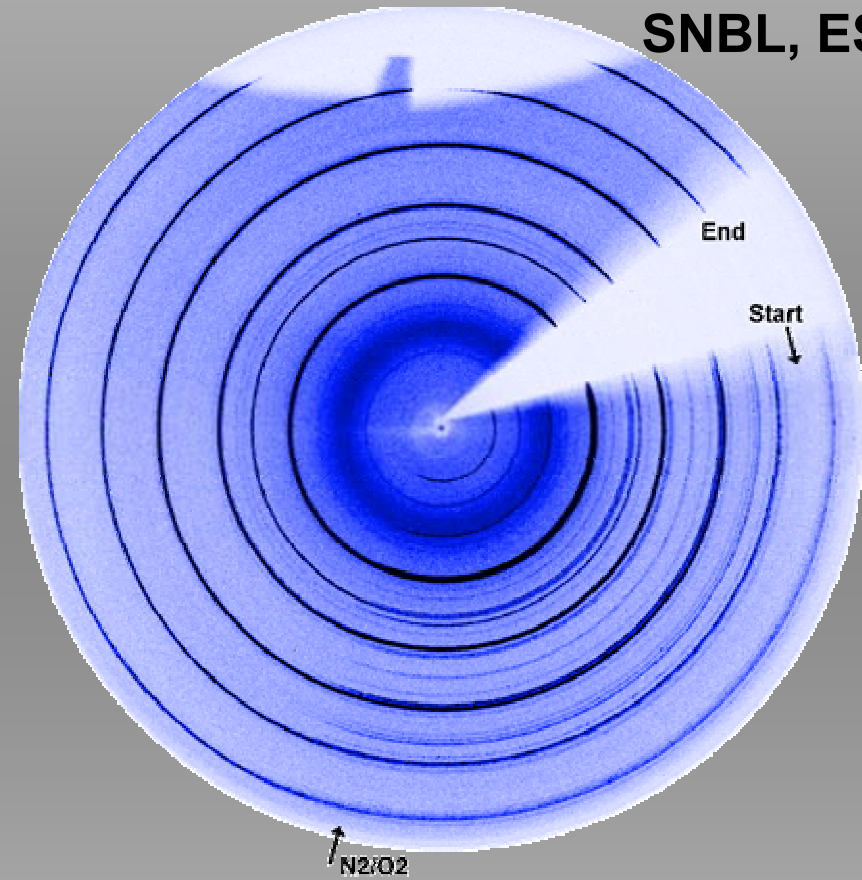
Challenge:

Determine the oxygen stoichiometry through an operating oxygen permeable membrane

- **The membrane is 10 mm in diameter and 2-3 mm thick**
- **Operating temperatures between 600 and 900°C**
- **Stable oxygen partial pressure gradient over the membrane**

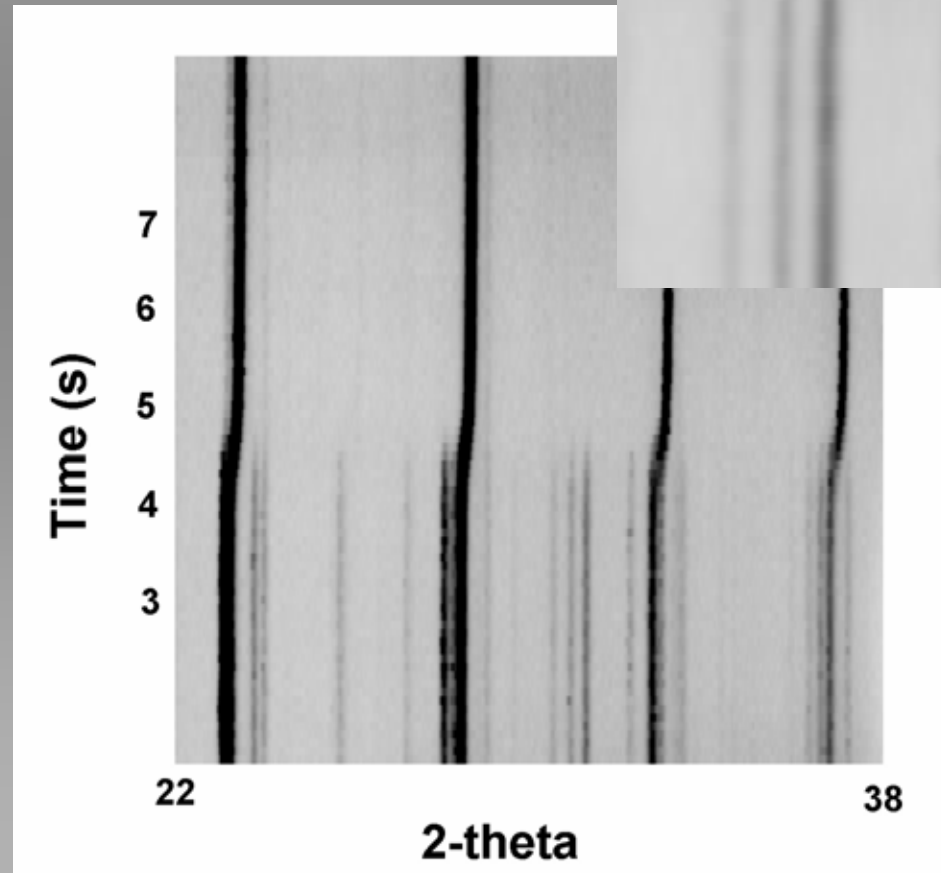
Time resolved in-situ studies of oxidation/reduction of $\text{SrFe}(\text{Cr})\text{O}_{3-\delta}$

SNBL, ESRF: Rotating Slit System



Oxidation of $\text{SrFe}(\text{Cr})\text{O}_{3-\delta}$

800°C , $\text{N}_2 \rightarrow \text{O}_2$



Fast Powder Diffraction using the Rotating Slit System

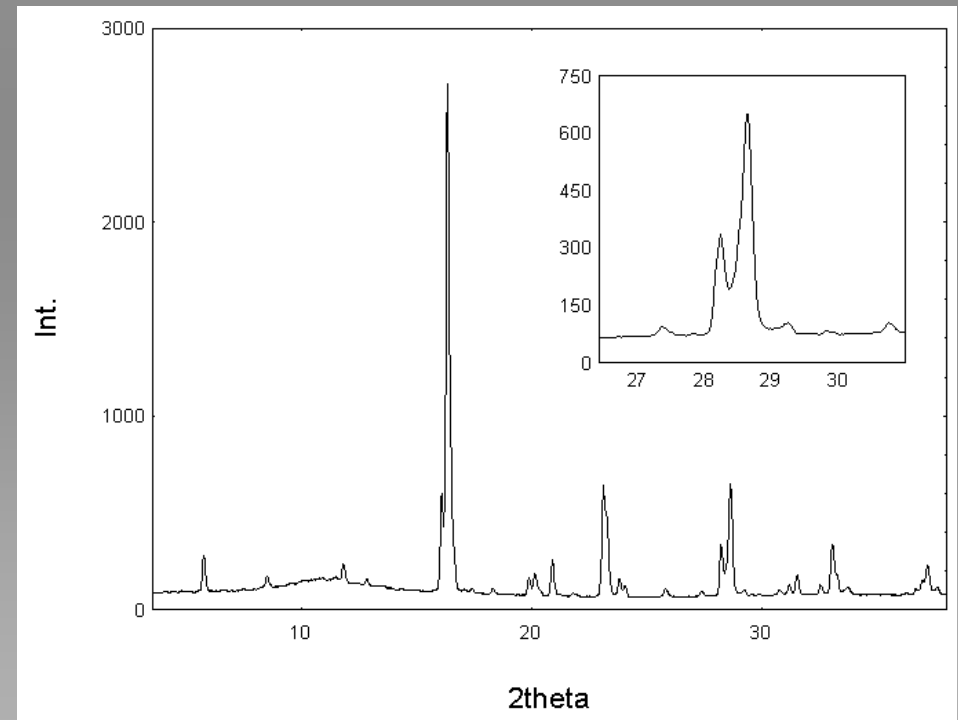
1/2 s. exposure time:

**Powder diffraction pattern
extracted during oxidation of
 $\text{SrFe}(\text{Cr})\text{O}_{3-\delta}$**

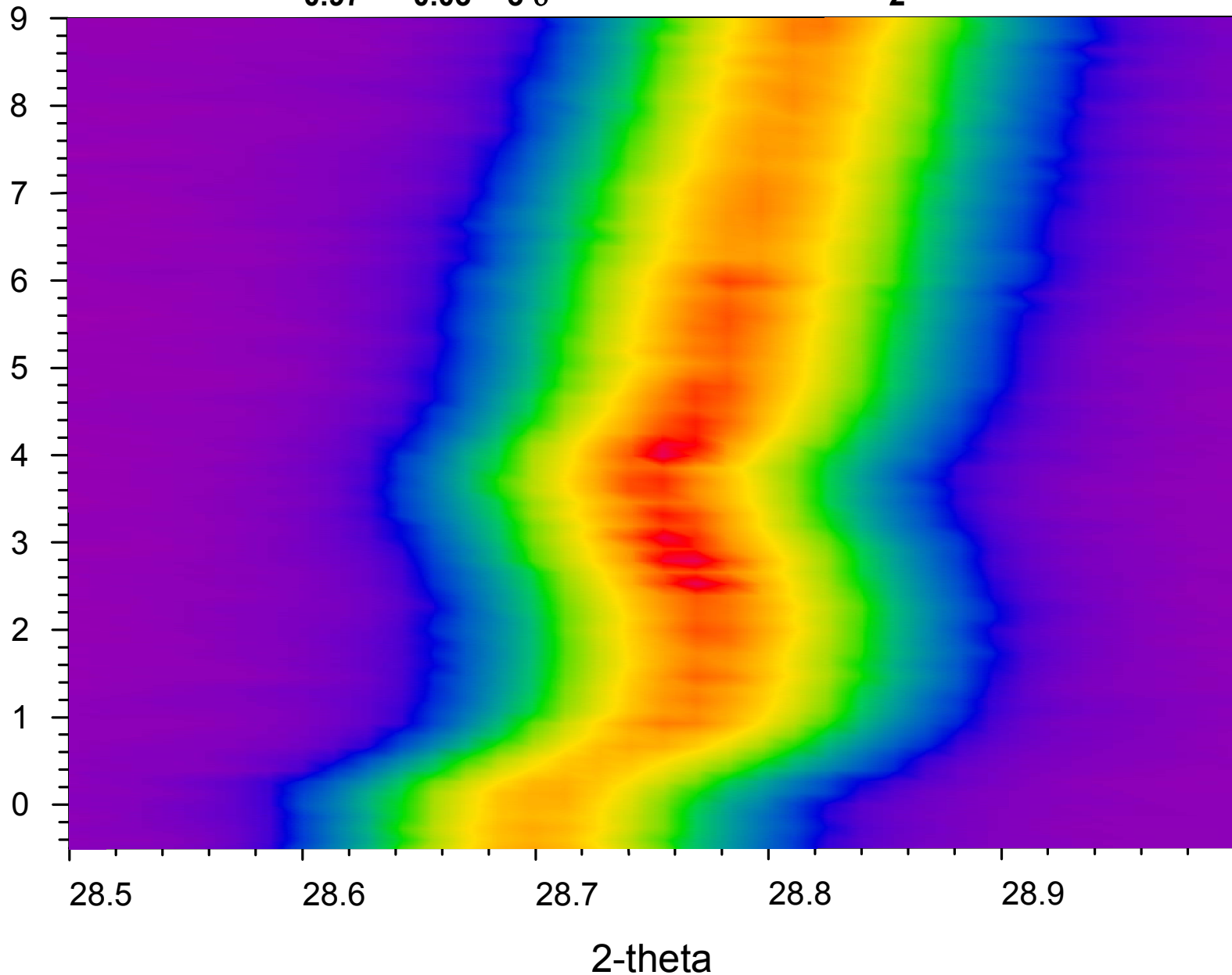
SNBL, ESRF

MAR345 Imaging Plate System

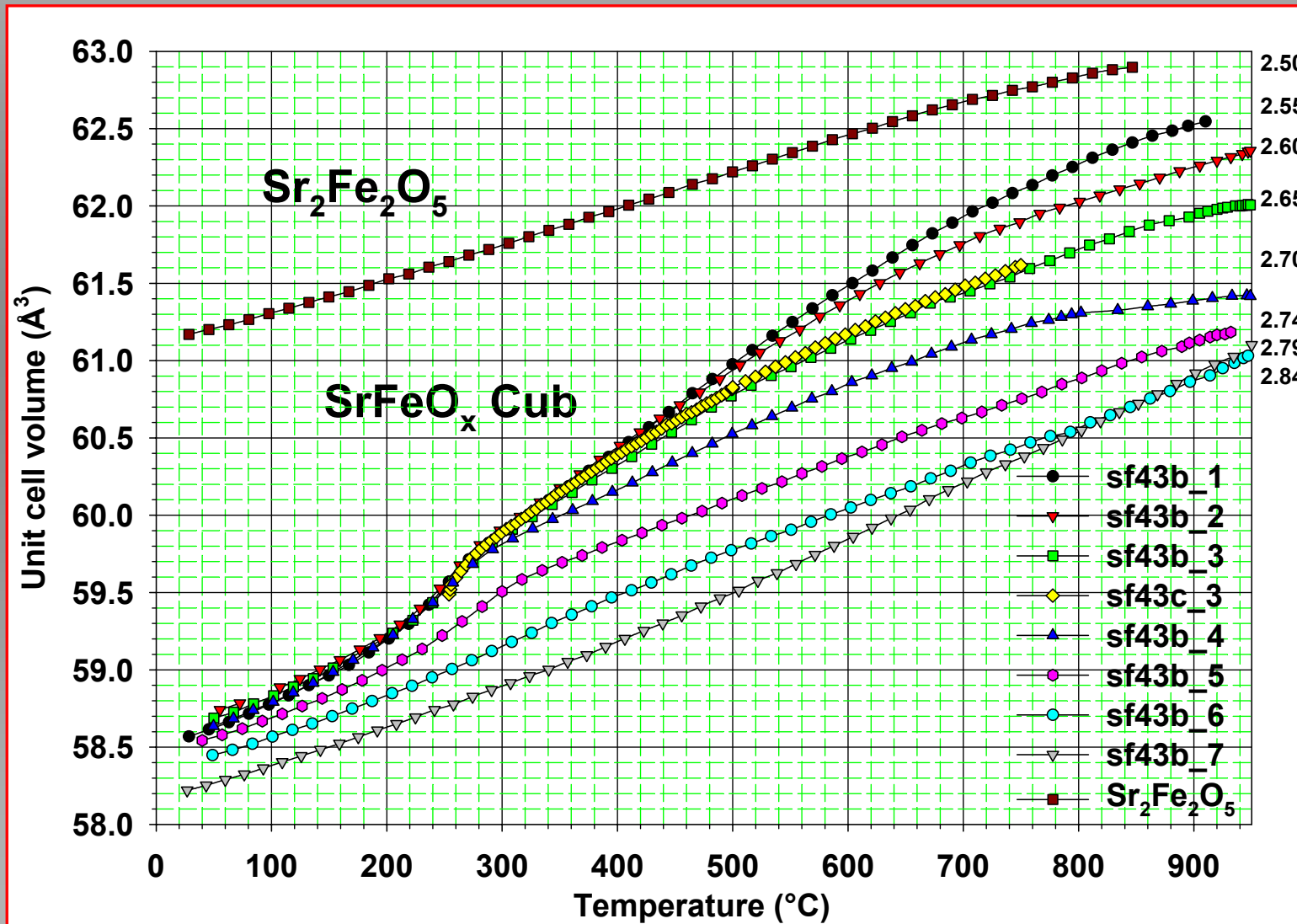
$\lambda = 0.7991\text{\AA}$



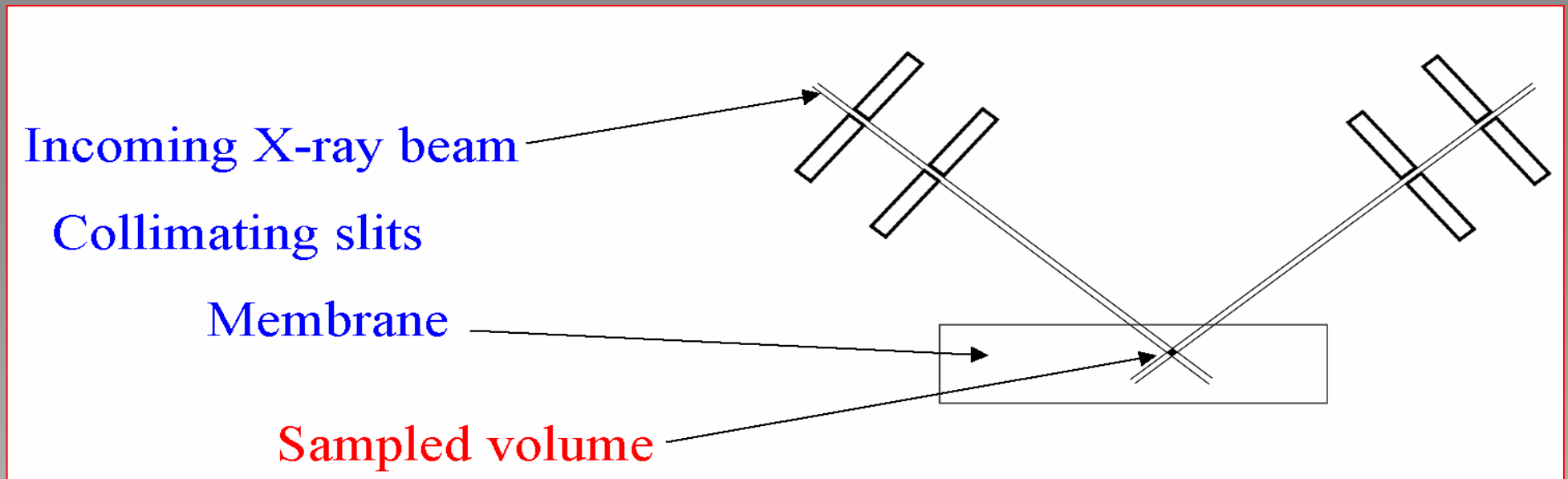
SrFe_{0.97}Cr_{0.03}O_{3-δ}, Oxidation in O₂ at 800°C



SrFe(Cr)O_x: Unit cell volume as a function of temperature and oxygen stoichiometry



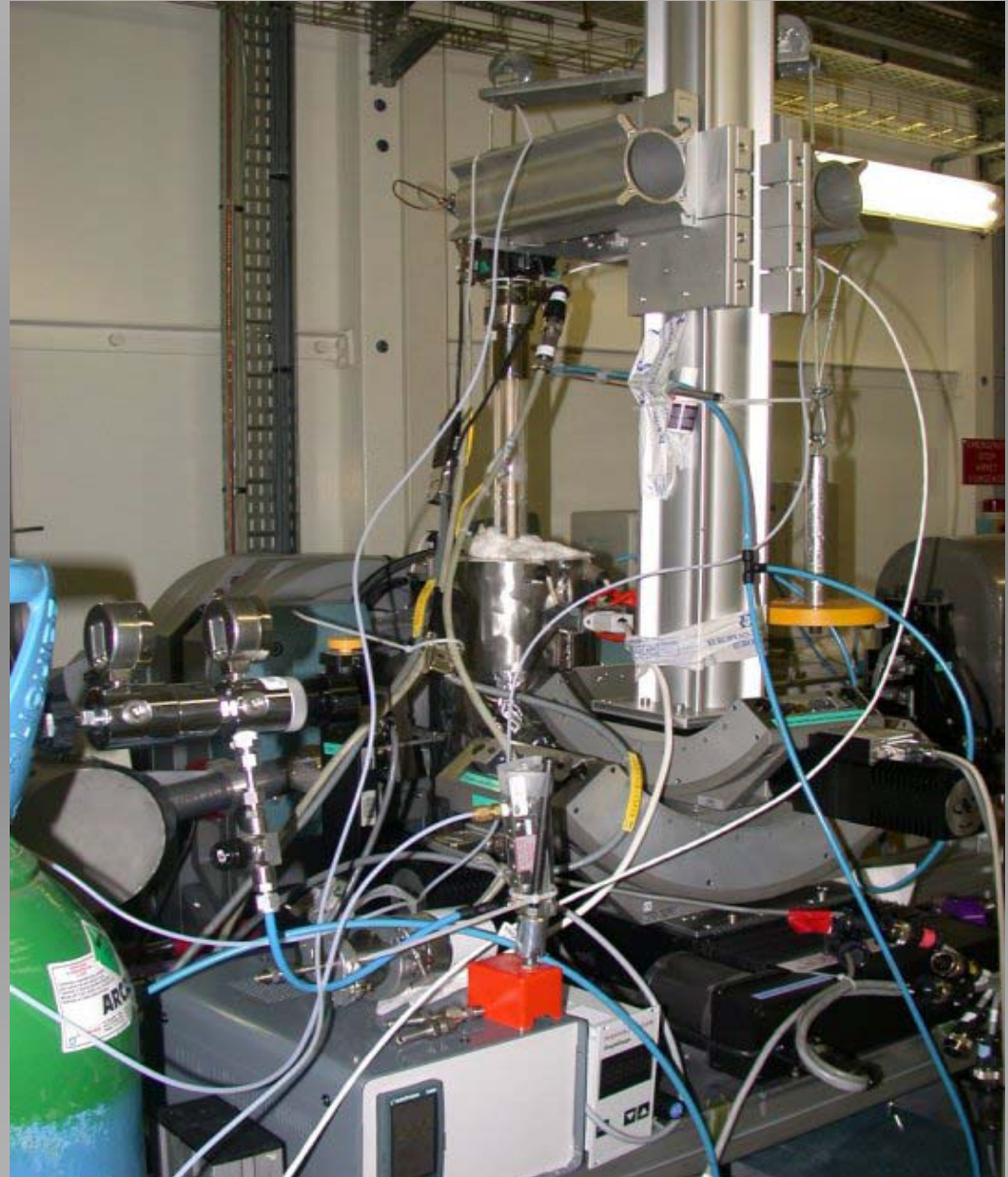
Principle of diffraction from a small volume element within a membrane.



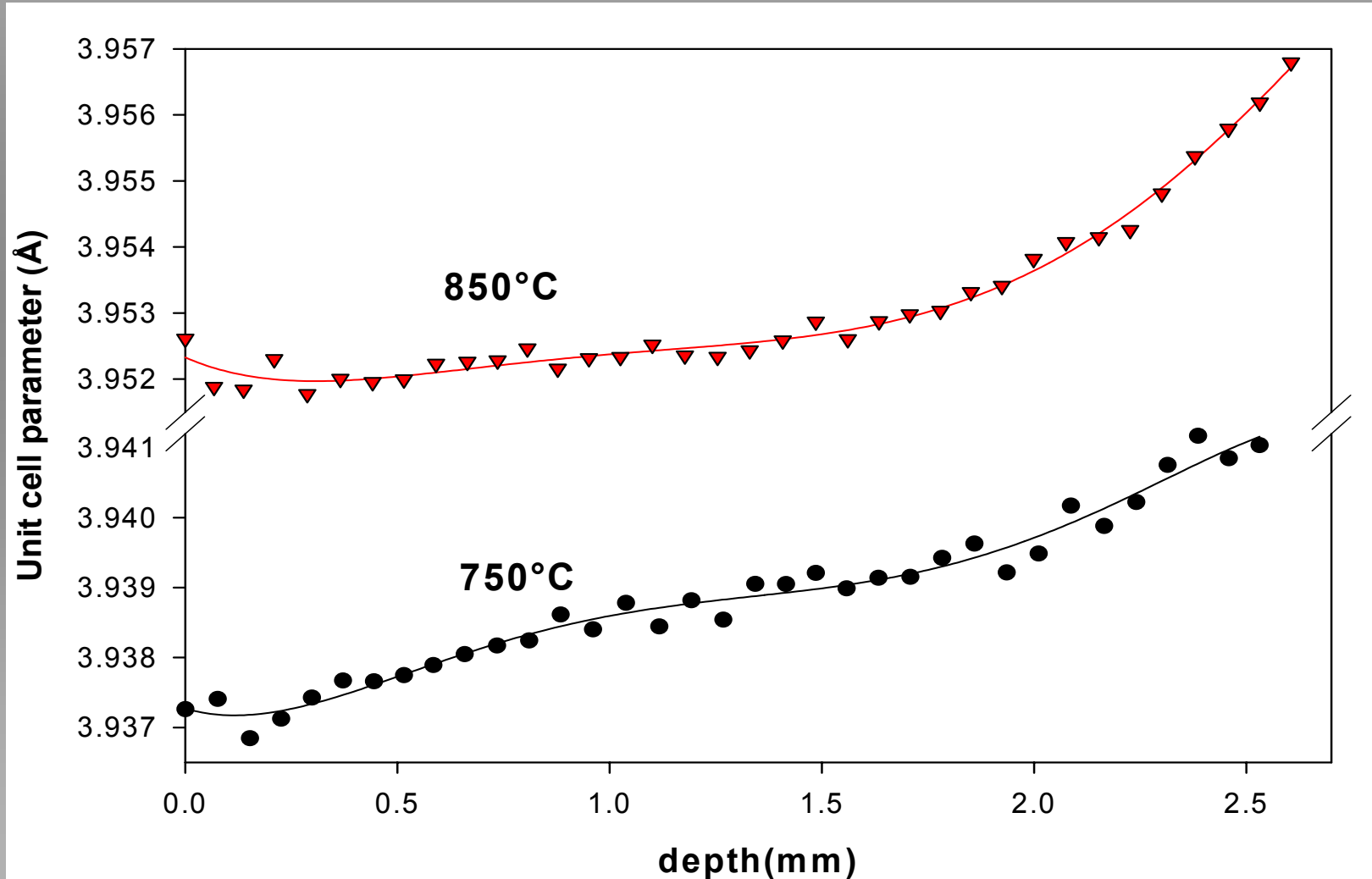
Experimental setup

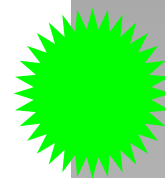
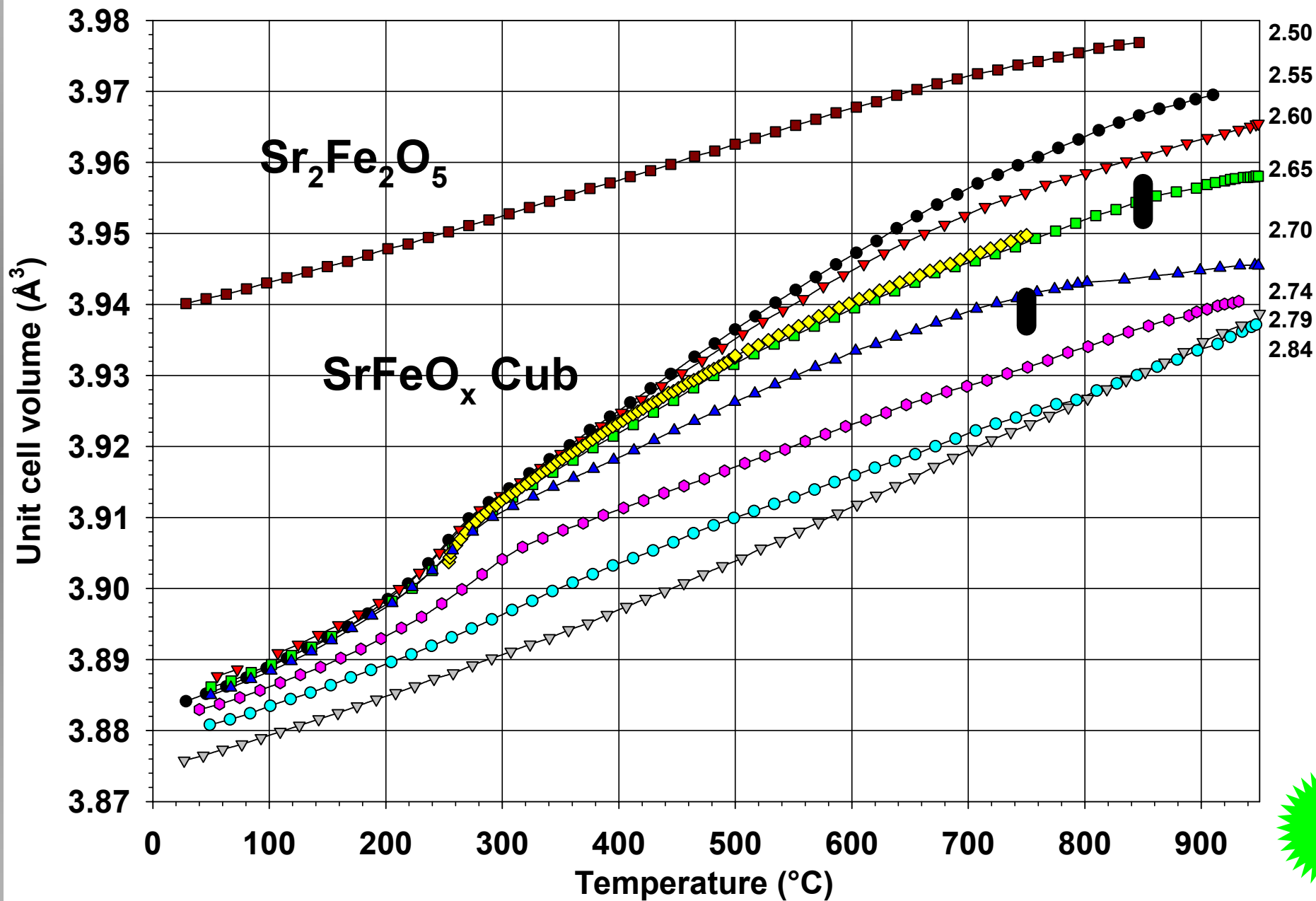
Materials Science
beamline

ID11
ESRF

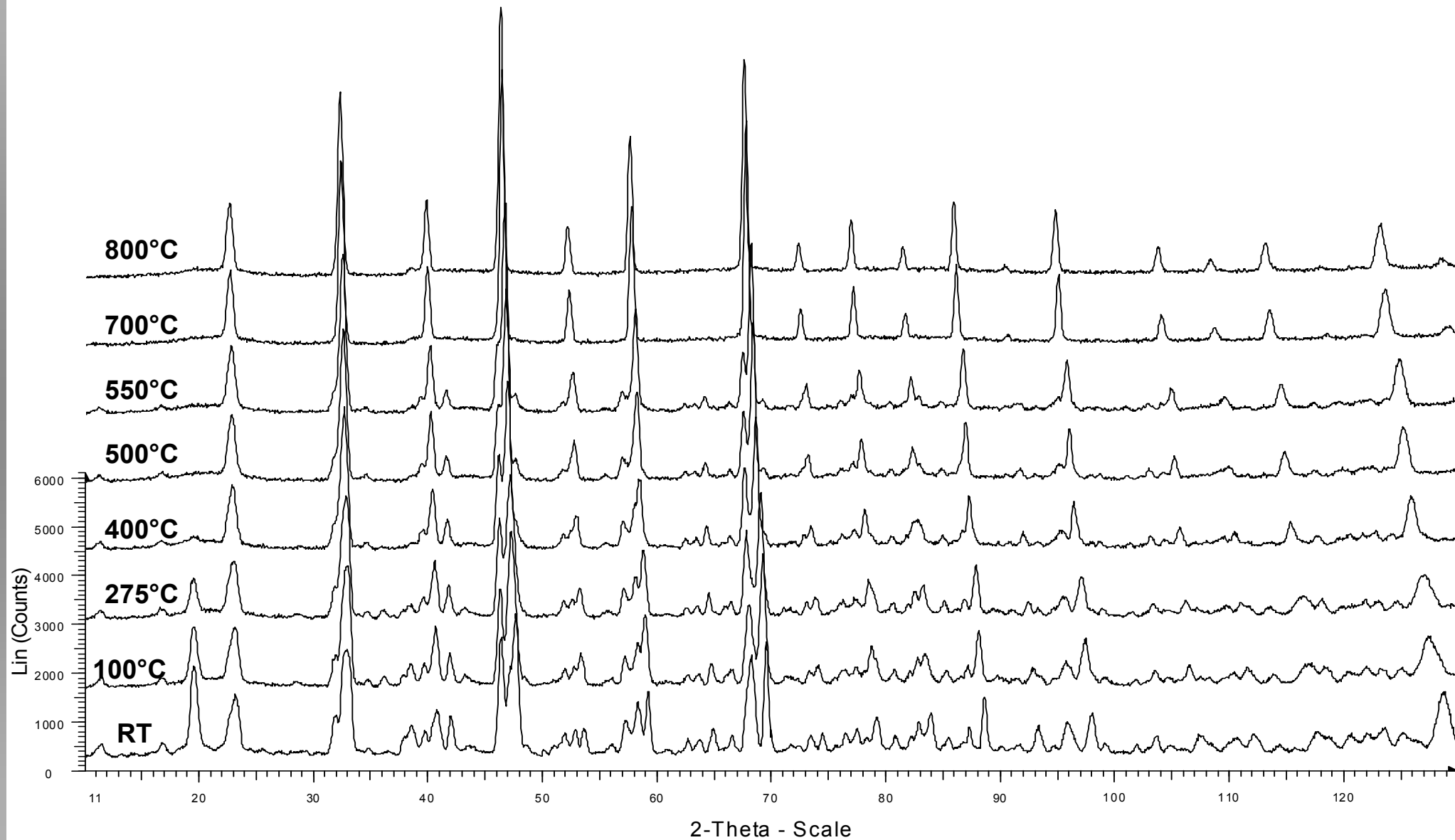


Experimentally determined cubic unit cell parameter through a 2.5 mm thick membrane ($\text{SrFe}_{0.97}\text{Cr}_{0.03}\text{O}_{3-\delta}$) at operating conditions.

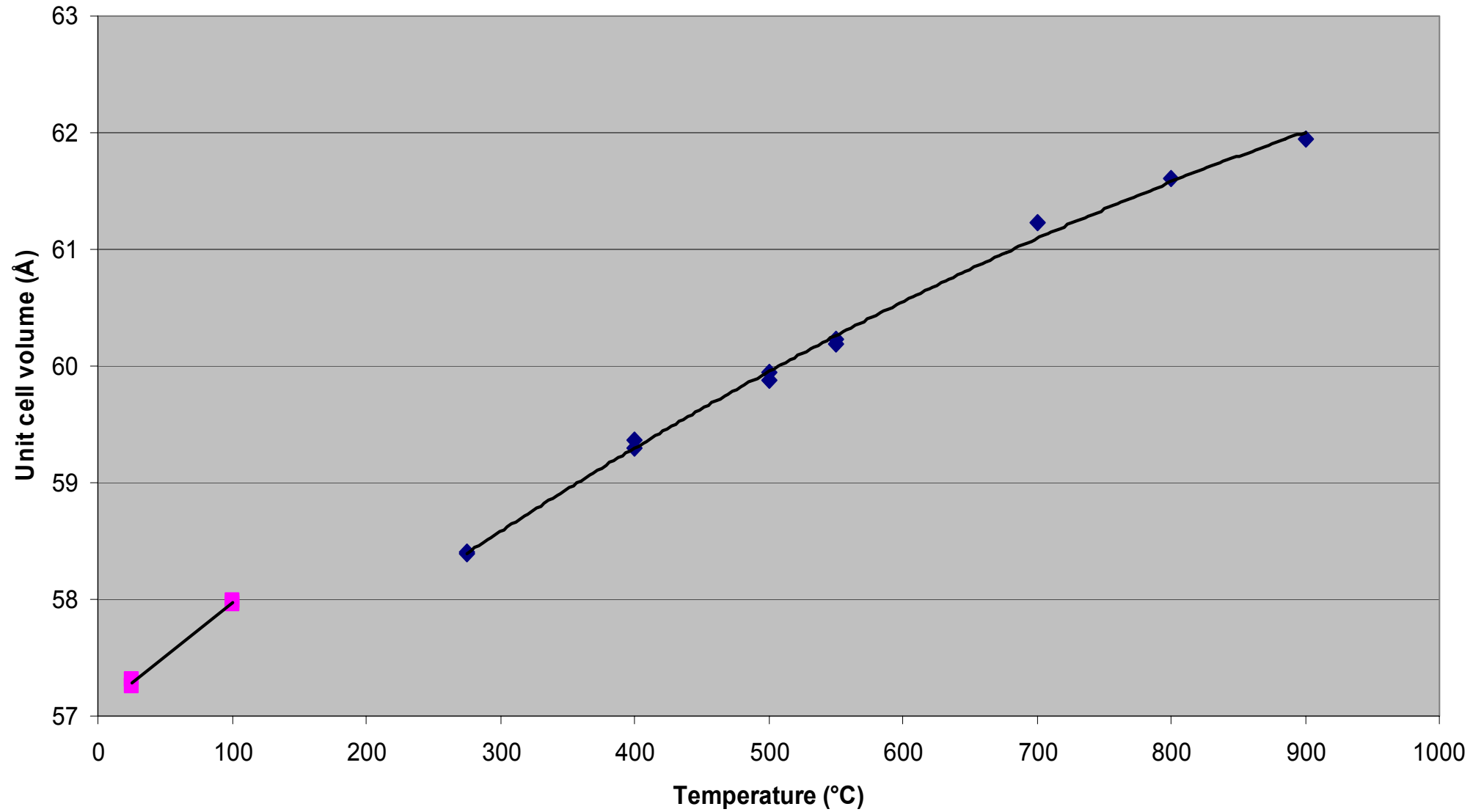




SrFeOx PUS Feb. 2005

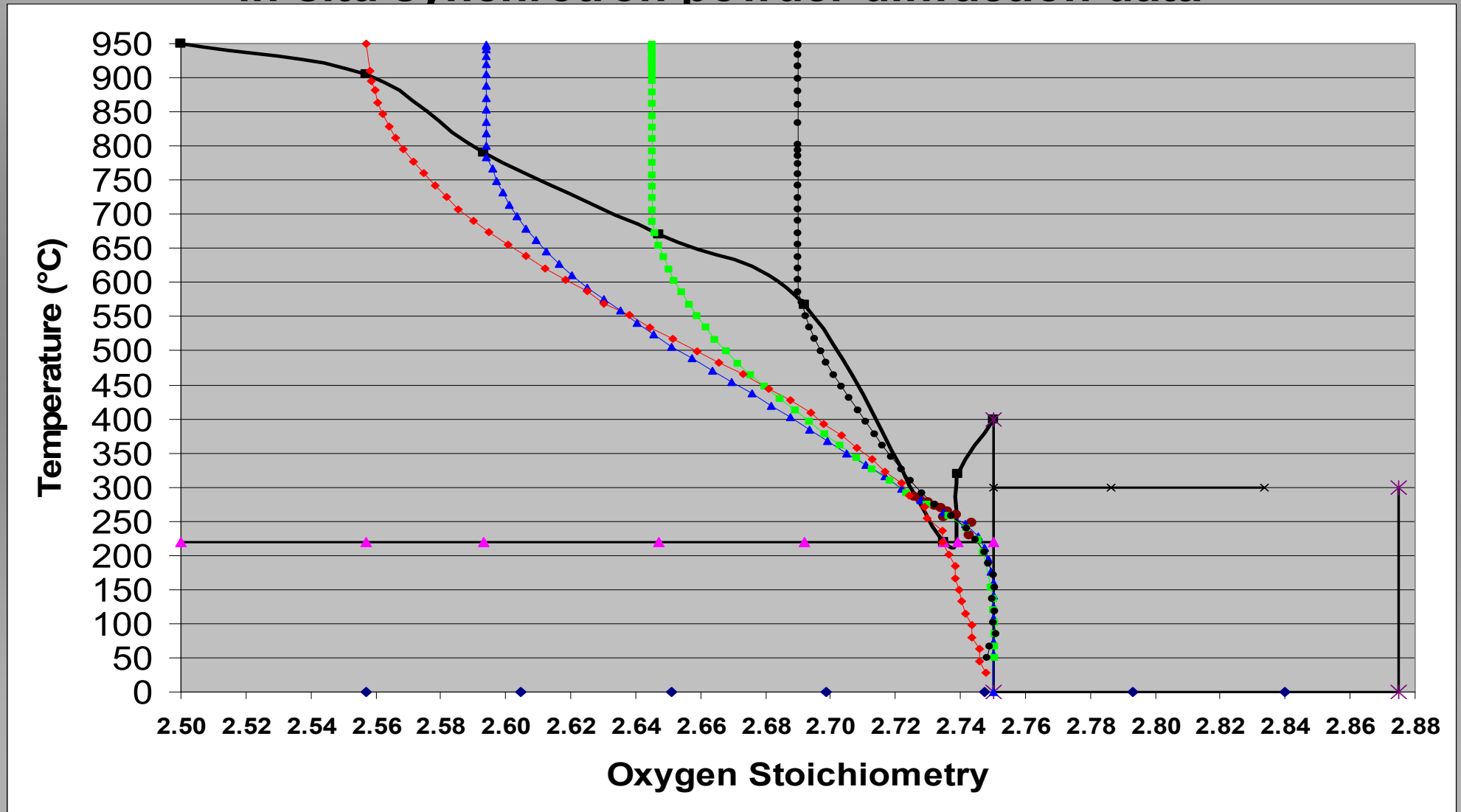


SrFeOx, reduced unit cell volume



SrFeO_x

Phase diagram determined by quantitative Rietveld refinement of in-situ synchrotron powder diffraction data



SrFeO_x

Phase diagram determined by quantitative Rietveld refinement of in-situ synchrotron powder diffraction data

